MATCH
Communications in Mathematical and in Computer Chemistry

MATCH Commun. Math. Comput. Chem. **58** (2007) 5-45

ISSN 0340 - 6253

Symmetry-Itemized Numbers of Alkanes as Stereoisomers

Shinsaku Fujita
Department of Chemistry and Materials Technology,
Kyoto Institute of Technology,
Matsugasaki, Sakyoku, Kyoto 606-8585, Japan
E-mail: fujitas@chem.kit.ac.jp

(Received February 14, 2007)

Abstract

Alkanes are counted as stereoisomers or three-dimensional trees (3D-trees) by means of Fujita's PCI (partial-cycle-index) method (Fujita, S., *Chem. Inf. Comput. Sci.*, **2000**, *40*, 135–146; Fujita, S., *Bull. Chem. Soc. Jpn.*, **2000**, *73*, 329–339) after they are categorized according to the dichotomy between centroidal and bicentroidal 3D-trees. The centroidal alkanes are enumerated by using a tetrahedral skeleton of $\mathbf{T}_d$-symmetry under the criterion of defining such centroidal 3D-trees, where they are itemized in terms of the eleven subgroups of the $\mathbf{T}_d$-symmetry. On the other hand, the bicentroidal alkanes are enumerated by using a two-nodal skeleton belonging to the **K**-symmetry, where they are itemized in terms of the five subgroups of the factor group $\mathbf{K} = \mathbf{D}_{\infty h}/\mathbf{C}_{\infty}$. Both the enumerations are based on functional equations derived from partial cycle indices with chirality fittingness, where the component functions $a(x^d)$, $c(x^d)$, and $b(x^d)$ (or their modifications) are substituted for three kinds of sphericity indices, i.e., a_d for homospheric orbits, c_d for enantiospheric orbits, and b_d for hemispheric orbits. Respective functional equations based on the itemization by subgroups are programmed by means of the Maple programming language. The resulting programs are executed to give respective stereoisomer numbers up to carbon content 100, which are collected in tabular forms with subgroup itemization.

1 Introduction

Manual enumeration of alkanes as constitutional isomers is one of elementary topics in an introductory course of organic chemistry, as found in most textbooks.[1–3] Although the enumeration is combined with the IUPAC nomenclature of alkanes as an introduction to the systematic nomenclature, it is not been described from stereochemical viewpoints. On the same line, combinatorial enumeration of alkanes has been conducted by regarding alkanes as constitutional isomers, as described in books[4–7] and reviews.[8–11] In the 1870s, a mathematician Cayley reported combinatorial enumeration of trees,[12, 13] which he already recognized to be models of alkanes in a chemical context. In the 1930s, Henze and Blair accomplished a more chemical investigation,[14, 15] were they used recursive equations in the enumeration of alkanes. Later in the 1930s, Pólya reported a systematic enumeration of alkanes as trees (constitutional isomers),[16, 17] where he used cycle indices (CIs) derived by a famous theorem bearing his name. Otter reported an alternative method for enumerating trees,[18] where he used his dissimilarity characteristic equation. Because these investigations depended on permutation-group theory which disregards inner structures of ligands, they did not properly treat stereochemical problems such as pseudoasymmetry and *meso*-compounds. More recently, Robinson et al. reported the enumeration of alkanes as stereoisomers,[19] where they used Pólya's cycle indices (CIs) and Otter's dissimilarity characteristic equations after modification. Even their treatment, however, took no account of the problems of pseudoasymmetry and *meso*-compounds because of disregard for the inner structures of ligands. Moreover, all of the previous works have not investigated symmetry-itemized enumeration of alkanes as stereoisomers.

By paying much regard to the inner structure of ligands, we have developed the USCI (unit-subduced-cycle-index) approach,[20] where we put emphasis on the concept of *sphericities of orbits*. Among the four methods provided by the USCI approach,[20–23] we have shown that the PCI (partial-cycle-index) method is especially useful because it gives generating functions itemized with point-group symmetries.[24, 25] We have developed an additional approach named the *proligand method*,[26–28] where we put emphasis on the concept of *sphericities of cycles*. The concept of *sphericities of orbits* in Fujita's USCI approach[20] and the concept of *sphericities of cycles* in Fujita's proligand method[26–28] are closely related to each other through the concept of *sphericities of orbits for cyclic groups* so that they are both capable of treating the inner structures of ligands properly and of solving the problems of pseudoasymmetry and *meso*-compounds.

In this paper, we discuss the aforementioned enumeration of alkanes as a probe for testifying the versatility of Fujita's PCI method, where the number of alkanes as stereoisomers is itemized so as to give respective numbers of point-group symmetries. In particular, PCI-CFs (partial cycle indices with chirality fittingness) derived by Fujita's PCI method are correlated to CI-CFs (cycle indices with chirality fittingness) derived by Fujita's proligand method.

2 Tetrahedral and Two-Nodal Promolecules

A promolecule is defined as a skeleton substituted by a set of proligands, which are in turn defined as structureless objects having chirality/achirality.[29] This section is devoted to examine tetrahedral promolecules and two-nodal promolecules.

2.1 Tetrahedral Promolecules

Tetrahedral promolecules are derived from a tetrahedral skeleton (**1**) belonging to the $\mathbf{T}_d$-point group.

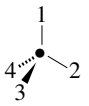

1

Figure 1: $\mathbf{T}_d$-skeleton (**1**) with four substitution positions. An solid circle (•) represents a carbon atom.

The four positions (1 to 4) of the tetrahedral skeleton (**1**) construct an orbit governed by a coset representation (CR) $\mathbf{T}_d(/\mathbf{C}_{3v})$. The corresponding unit subduced cycle indices with chirality fittingness (USCI-CFs)[30, 31] have been derived from the CRs and collected in the $\mathbf{T}_d(/\mathbf{C}_{3v})$-row of Appendix E.10 of Fujita's book,[20] which is cited as a tentative row vector:

$$(b_1^4, b_2^2, a_1^2c_2, b_1b_3, c_4, b_4, a_2^2, a_1a_3, a_4, b_4, a_4). \tag{1}$$

According to Theorem 19.7 of Fujita's book,[20] this vector is multiplied by the inverse mark table for $\mathbf{T}_d$ listed in Appendix B.1 of the same book to give the corresponding PCI-CFs as follows:[25]

$$\begin{aligned}
\text{PCI-CF}(\mathbf{C}_1, \$_d) &= \frac{1}{24}b_1^4 - \frac{1}{8}b_2^2 - \frac{1}{4}a_1^2c_2 - \frac{1}{6}b_1b_3 + \frac{1}{12}b_4 \\
&\quad + \frac{1}{4}a_2^2 + \frac{1}{2}a_1a_3 + \frac{1}{6}b_4 - \frac{1}{2}a_4 && (2)\\
\text{PCI-CF}(\mathbf{C}_2, \$_d) &= \frac{1}{4}b_2^2 - \frac{1}{4}c_4 - \frac{1}{4}b_4 - \frac{1}{4}a_2^2 + \frac{1}{2}a_4 && (3)\\
\text{PCI-CF}(\mathbf{C}_s, \$_d) &= \frac{1}{2}a_1^2c_2 - \frac{1}{2}a_2^2 - a_1a_3 + a_4 && (4)\\
\text{PCI-CF}(\mathbf{C}_3, \$_d) &= \frac{1}{2}b_1b_3 - \frac{1}{2}a_1a_3 - \frac{1}{2}b_4 + \frac{1}{2}a_4 && (5)\\
\text{PCI-CF}(\mathbf{S}_4, \$_d) &= \frac{1}{2}c_4 - \frac{1}{2}a_4 && (6)\\
\text{PCI-CF}(\mathbf{D}_2, \$_d) &= 0 && (7)\\
\text{PCI-CF}(\mathbf{C}_{2v}, \$_d) &= \frac{1}{2}a_2^2 - \frac{1}{2}a_4 && (8)\\
\text{PCI-CF}(\mathbf{C}_{3v}, \$_d) &= a_1a_3 - a_4 && (9)\\
\text{PCI-CF}(\mathbf{D}_{2d}, \$_d) &= 0 && (10)\\
\text{PCI-CF}(\mathbf{T}, \$_d) &= \frac{1}{2}b_4 - \frac{1}{2}a_4 && (11)\\
\text{PCI-CF}(\mathbf{T}_d, \$_d) &= a_4, && (12)
\end{aligned}$$

where the symbol \$ represents a, b, or c. These equations count each achiral promolecule just once and each enantiomeric pair of chiral promolecules just once. By summing up

eqs. 2–12, we obtain the following cycle index with chirality fittingness (CI-CF):

$$\text{CI-CF}(\mathbf{T}_d, \$_d) = \frac{1}{24}b_1^4 + \frac{1}{8}b_2^2 + \frac{1}{3}b_1b_3 + \frac{1}{4}a_1^2c_2 + \frac{1}{4}c_4. \tag{13}$$

which is identical with the CI-CF derived by Fujita's proligand method.[26–28]

Let us consider achiral proligands X, Y, Z, and H as well as chiral proligands p/$\overline{\text{p}}$, q/$\overline{\text{q}}$, and r/$\overline{\text{r}}$ (enantiomeric pairs of chiral proligands), which are used as substituents for the $\mathbf{T}_d$-skeleton (**1**), i.e.,

$$\mathbf{X} = \{\text{X}, \text{Y}, \text{Z}, \text{H}; \text{p}, \overline{\text{p}}; \text{q}, \overline{\text{q}}; \text{r}, \overline{\text{r}}; \text{s}, \overline{\text{s}}\}. \tag{14}$$

Suppose that a set of proligands is selected from the proligand warehouse $\mathbf{X}$ (eq. 14) to give a tetrahedral derivative, Then, the following ligand inventories are calculated:

$$a_d = \text{X}^d + \text{Y}^d + \text{Z}^d + \text{H}^d \tag{15}$$

$$c_d = \text{X}^d + \text{Y}^d + \text{Z}^d + \text{H}^d + 2\text{p}^{d/2}\overline{\text{p}}^{d/2} + 2\text{q}^{d/2}\overline{\text{q}}^{d/2} + 2\text{r}^{d/2}\overline{\text{r}}^{d/2} + 2\text{s}^{d/2}\overline{\text{s}}^{d/2} \tag{16}$$

$$b_d = \text{X}^d + \text{Y}^d + \text{Z}^d + \text{H}^d + \text{p}^d + \overline{\text{p}}^d + \text{q}^d + \overline{\text{q}}^d + \text{r}^d + \overline{\text{r}}^d + \text{s}^d + \overline{\text{s}}^d. \tag{17}$$

These ligand inventories are introduced to the PCI-CFs (eqs. 2–12) to give generating functions for counting the respective numbers of promolecules.[32] Some of the generating functions are shown as follows:

$$f_{\mathbf{C}_2} = [\frac{1}{2}(\text{X}^2\text{p}^2 + \text{X}^2\overline{\text{p}}^2) + \frac{1}{2}(\text{X}^2\text{q}^2 + \text{X}^2\overline{\text{q}}^2) + \cdots] + [\frac{1}{2}(\text{p}^2\text{q}^2 + \overline{\text{p}}^2\overline{\text{q}}^2) + \frac{1}{2}(\text{p}^2\text{r}^2 + \overline{\text{p}}^2\overline{\text{r}}^2) + \cdots] \tag{18}$$

$$f_{\mathbf{C}_s} = (\text{X}^2\text{YZ} + \text{X}^2\text{ZH} + \cdots) + (\text{X}^2\text{p}\overline{\text{p}} + \text{X}^2\text{q}\overline{\text{q}} + \cdots) + (2\text{XYp}\overline{\text{p}} + 2\text{XYq}\overline{\text{q}} + \cdots). \tag{19}$$

Such a term as $(1/2)(\text{X}^2\text{p}^2 + \text{X}^2\overline{\text{p}}^2)$ represents a pair of enantiomers, which is counted just once. Such a term as $\text{X}^2\text{p}\overline{\text{p}}$ represents a so-called *meso*-like compound, which is counted just once as an achiral stereoisomer. Note that the term XYZH is used in place of (1/2)[XYZH(right) + $\overline{\text{XYZH}}$(left)] on the basis of the model adopted in the present enumeration. The results due to the PCI method (e.g., eqs. 18 and 19) are identical with those based on the subduced-cycle-index (SCI) method reported previously.[29] For the sake of convenience for further discussions, the structures of promolecules are cited from Chapter 21 of Fujita's book,[20] as shown in Fig. 2. Note that each promolecule in Fig. 2 is selected as a representative of promolecules of the same type. For examples, the promolecule **2** having X^4 is a representative of promolecules having X^4, Y^4, Z^4, H^4, and so on.

2.2 Two-Nodal Promolecules

To treat *meso*-compounds properly, we shall regard them as derivatives of a two-nodal skeleton (**39**) with two substituents. The two-nodal skeleton (**39**) belongs to a point group of infinite order, i.e., $\mathbf{D}_{\infty h}$.

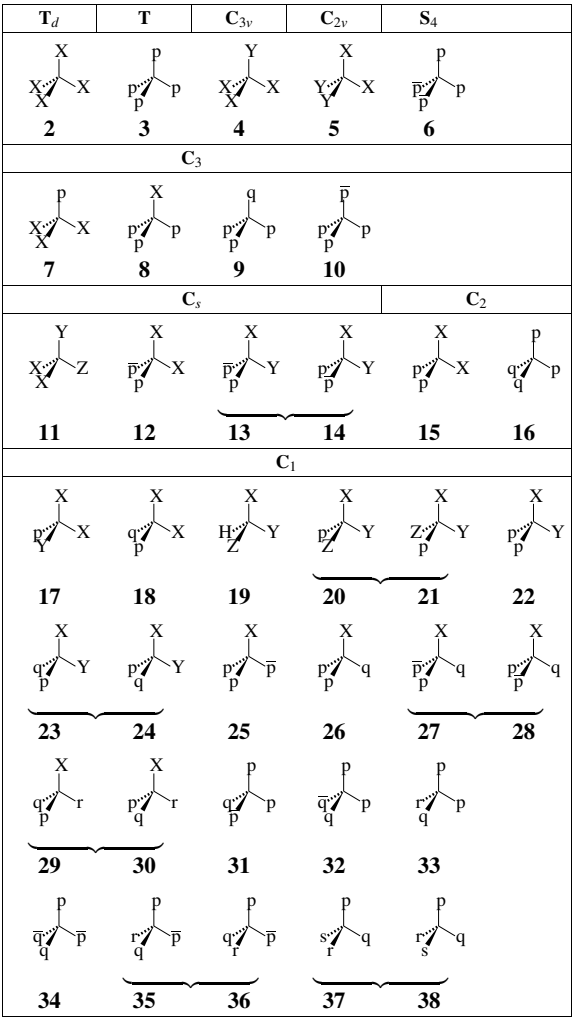

Figure 2: Promolecules for centroidal 3D-trees, which are derived from a tetrahedral skeleton of $\mathbf{T}_d$-symmetry.[29, 20] The symbols X, Y, Z, and H represent achiral proligands, while the symbols p/$\overline{\text{p}}$, q/$\overline{\text{q}}$, r/$\overline{\text{q}}$, and s/$\overline{\text{s}}$ represent enantiomeric pairs of chiral proligands. Either one selected from an enantiomeric pair of promolecules is depicted as a representative.

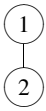

39

Figure 3: $\mathbf{D}_{\infty h}$-skeleton or $\mathbf{D}_{\infty h}/\mathbf{C}_{\infty}$-skeleton (**39**) with two substitution positions.

Because the $\mathbf{D}_{\infty h}$ is not easy to treat because of its infinite nature, we adopt the corresponding factor group $\mathbf{D}_{\infty h}/\mathbf{C}_{\infty}$ ($= \mathbf{K}$). According to the treatment reported previously,[33] the factor group $\mathbf{K}$ represented by a set of cosets:

$$\mathbf{K} = \mathbf{D}_{\infty h}/\mathbf{C}_{\infty} = \{\mathbf{C}_{\infty}I, \mathbf{C}_{\infty}C_2, \mathbf{C}_{\infty}\sigma_v, \mathbf{C}_{\infty}\sigma_h\}, \tag{20}$$

which has five subgroups as follows:

$$\begin{aligned}
\mathbf{K}_1 &= \mathbf{C}_{\infty}/\mathbf{C}_{\infty} = \{\mathbf{C}_{\infty}I\} && (21)\\
\mathbf{K}_2 &= \mathbf{D}_{\infty}/\mathbf{C}_{\infty} = \{\mathbf{C}_{\infty}I, \mathbf{C}_{\infty}C_2\} && (22)\\
\mathbf{K}_3 &= \mathbf{C}_{\infty v}/\mathbf{C}_{\infty} = \{\mathbf{C}_{\infty}I, \mathbf{C}_{\infty}\sigma_v\} && (23)\\
\mathbf{K}_4 &= \mathbf{C}_{\infty h}/\mathbf{C}_{\infty} = \{\mathbf{C}_{\infty}I, \mathbf{C}_{\infty}\sigma_h\} && (24)\\
\mathbf{K}_5 &= \mathbf{K} = \mathbf{D}_{\infty h}/\mathbf{C}_{\infty}. && (25)
\end{aligned}$$

Thereby, the $\mathbf{D}_{\infty h}$-skeleton (**39**) is regarded as a $\mathbf{D}_{\infty h}/\mathbf{C}_{\infty}$-skeleton, where its two positions belong to an orbit governed by the CR $\mathbf{K}(/\mathbf{K}_3)$. Because the factor group $\mathbf{K}$ is isomorphic to the point group $\mathbf{C}_{2v}$, we can use the correspondence of subgroups:

$$\begin{aligned}
\mathbf{K}_1 &\sim \mathbf{C}_1 = \{I\} && (26)\\
\mathbf{K}_2 &\sim \mathbf{C}_2 = \{I, C_2\} && (27)\\
\mathbf{K}_3 &\sim \mathbf{C}_s = \{I, \sigma_{v(1)}\} && (28)\\
\mathbf{K}_4 &\sim \mathbf{C}'_s = \{I, \sigma_{v(2)}\} && (29)\\
\mathbf{K}_5 &\sim \mathbf{C}_{2v} = \{I, C_2, \sigma_{v(1)}, \sigma_{v(2)}\}. && (30)
\end{aligned}$$

This means that where we can use the CR $\mathbf{C}_{2v}(/\mathbf{C}_s)$ in place of the CR $\mathbf{K}(/\mathbf{K}_3)$, if necessary. By following the USCI approach [34, 25] the PCI-CFs for the subgroups listed in eqs. 21–25 are obtained as follows:[34]

$$\begin{aligned}
\text{PCI-CF}(\mathbf{K}_1, \$_d) &= \frac{1}{4}b_1^2 - \frac{1}{4}b_2 - \frac{1}{4}a_1^2 - \frac{1}{4}c_2 + \frac{1}{2}a_2 && (31)\\
\text{PCI-CF}(\mathbf{K}_2, \$_d) &= \frac{1}{2}b_2 - \frac{1}{2}a_2 && (32)\\
\text{PCI-CF}(\mathbf{K}_3, \$_d) &= \frac{1}{2}a_1^2 - \frac{1}{2}a_2 && (33)\\
\text{PCI-CF}(\mathbf{K}_4, \$_d) &= \frac{1}{2}c_2 - \frac{1}{2}a_2 && (34)\\
\text{PCI-CF}(\mathbf{K}, \$_d) &= a_2, && (35)
\end{aligned}$$

where we use the USCI-CF table and the inverse table of marks for the isomorphic group $\mathbf{C}_{2v}$ (Appendices E.5 and B.5 of Fujita's book[20]).

By summing up the PCI-CF shown in eqs. 31–35, we obtain the following CI-CF:

$$\text{CI-CF}(\mathbf{K};\$_d) = \frac{1}{4}\left(b_1^2 + b_2 + a_1^2 + c_2\right). \tag{36}$$

This CI-CF is identical with the one derived by means of Fujita's proligand method,[26–28] although the SIs in eq. 36 are concerned with the sphericities of orbits of cycle subgroups, while the SIs in the CI-CF of Fujita's proligand method are concerned with the sphericities of cycles.

Suppose that we select two proligands from achiral proligands (X and Y) and chiral proligands (p, $\overline{\text{p}}$, q, and $\overline{\text{q}}$), where p and $\overline{\text{p}}$ (or q and $\overline{\text{q}}$) represent a pair of enantiomeric proligands in isolation. By following Theorem 1 of the previous paper,[26] we use the following inventories:

$$a_d = \text{X}^d + \text{Y}^d \tag{37}$$

$$c_d = \text{X}^d + \text{Y}^d + 2\text{p}^{d/2}\overline{\text{p}}^{d/2} + 2\text{q}^{d/2}\overline{\text{q}}^{d/2} \tag{38}$$

$$b_d = \text{X}^d + \text{Y}^d + \text{p}^d + \overline{\text{p}}^d + q^d + \overline{q}^d. \tag{39}$$

In the present case, promolecules to be examined are not so complicated that the itemization based on eqs. 31–35 is overprescribed to discuss symmetrical features of two-nodal promolecules. Hence we use eq. 36 for obtaining the total number. The inventories (eqs. 37–39) are introduced into eq. 36 and the resulting equation is expanded to give the following generating function:

$$\begin{aligned} F = {} & [\text{X}^2 + \text{Y}^2] + [\text{XY}] + [\text{p}\overline{\text{p}} + \text{q}\overline{\text{q}}] \\ & + \frac{1}{2}[(\text{p}^2 + \overline{\text{p}}^2) + (\text{q}^2 + \overline{\text{q}}^2)] \\ & + \frac{1}{2}[(\text{Xp} + \text{X}\overline{\text{p}}) + (\text{Xq} + \text{X}\overline{\text{q}}) + (\text{Yp} + \text{Y}\overline{\text{p}}) + (\text{Yq} + \text{Y}\overline{\text{q}})] \\ & + \frac{1}{2}[(\text{pq} + \overline{\text{pq}}) + (\text{p}\overline{\text{q}} + \overline{\text{p}}\text{q}], \end{aligned} \tag{40}$$

where the coefficient of each term represents the number of promolecules based on the **K**-skeleton (**39**). The promolecules are depicted in Fig. 4, where a representative of each type of promolecules is depicted with its symmetry specification. Note that each of the representatives corresponds to a set of terms in each pair of brackets in the right-hand side of eq. 40.

3 Alkyl Ligands as Proligands

In the next step, we shall convert the tetrahedral promolecules (Subsection 2.1) and the two-nodal promolecules (Subsection 2.2) into alkanes, where the proligands listed in the proligand warehouse **X** (eq. 14) are replaced by adequate alkyl ligands.

To accomplish this conversion, suppose that an alkyl ligand is characterized by its carbon content k and that the number of such alkyl ligands as having carbon content k is represented as the coefficient of the term x^k. Thereby, the set of PCI-CFs for tetrahedral

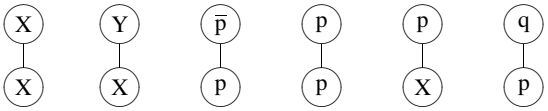

40 (**K**) **41** (**K**$_3$) **42** (**K**$_4$) **43** (**K**$_2$) **44** (**K**$_1$) **45** (**K**$_1$)

Figure 4: Promolecules based on the skeleton **39**. The promolecules X—X, X—Y, and p—$\overline{\text{p}}$ are achiral. The other promolecules X—p, p—p, and p—q are chiral, where an appropriate enantiomer is depicted for each pair of enantiomers.

derivatives (eqs. 2–12) and the set of PCI-CFs for two-nodal derivatives (eqs. 31–35) are evaluated by considering that the SIs a_d, c_d, and b_d in the two sets of PCI-CFs are represented by using respective counting series $a(x^d)$, $c(x^d)$, and $d(x^d)$, where we use the symbols $a(x)$, $c(x)$, and $b(x)$ to represent generating functions for counting respective numbers:

$$a(x) = \sum_{k=0}^{\infty} \alpha_k x^k \tag{41}$$

$$c(x^2) = \sum_{k=0}^{\infty} \gamma_k x^{2k} \tag{42}$$

$$b(x) = \sum_{k=0}^{\infty} \beta_k x^k. \tag{43}$$

In the derivation of these equations, we have taken account of the ligand inventories shown in eqs. 15–17 and eqs. 37–39. Hence, the coefficient (α_k) of the term x^k in the counting series $a(x)$ represents the number of achiral alkyl ligands (or planted 3D-trees) of carbon content k; that the coefficient (γ_k) of the term x^{2k} in the counting series $c(x^2)$ represents the number of diploids of carbon content $2k$, in which an achiral alkyl ligand or a pair of enantiomeric alkyl ligands (or planted 3D-trees) is counted once; and finally that the coefficient (β_k) of the term x^k in the counting series $b(x)$ represents the number of achiral and chiral alkyl ligands (or planted 3D-trees) of carbon content k, in which two enantiomers of each pair are separately counted. We put $\alpha_0 = 1$, $\gamma_0 = 1$, and $\beta_0 = 1$ to treat trivial cases of terminal vertices (or hydrogen atoms).

To evaluate eqs. 41–43, we consider a $\mathbf{C}_{3v}$-skeleton (**46**) in which the three positions (1–3) construct an orbit governed by a coset representation (CR) $\mathbf{C}_{3v}(/\mathbf{C}_s)$. The positions accommodate a set of proligands, e.g., X, Y, and Z, to give another proligand, which is regarded as a planted promolecule (**47**). When we place X = CH_3, Y = CH_2CH_3, and Z = $CH_2CH_2CH_3$, we obtain a chiral alkyl ligand (3-methylhex-3-yl ligand). Each of the inner proligands (X, Y, and Z) is regarded as a planted promolecule in a nested fashion. For example, the proligand Z = $CH_2CH_2CH_3$ is in turn regarded as being derived from the $\mathbf{C}_{3v}$-skeleton (**46**) by the substitution of two hydrogens and a proligand Y (= CH_2CH_3); and then the proligand Y = CH_2CH_3 is in turn regarded as being derived from the $\mathbf{C}_{3v}$-skeleton (**46**) by the substitution of two hydrogens and a proligand X (= CH_3). In general, this recursive process can be applied to any proligands, which can be finally reduced into a methyl ligand. It should be emphasized that each of the intermediate proligands (as

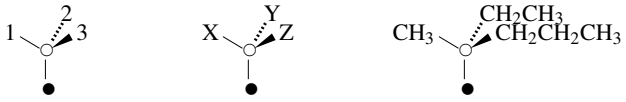

46 | **47** | **48**

$\mathbf{C}_{3v}$-skeleton ($\mathbf{C}_{3v}(/\mathbf{C}_s)$) | proligand planted promolecule | alkyl ligand planted 3D-tree

Figure 5: $\mathbf{C}_{3v}$-skeleton (**46**) with three substitution positions, a proligand as a planted promolecule (**47**), and an alkyl ligand (3-methylhex-3-yl ligand) as a planted 3D-tree (**48**). A solid circle (•) represents a root, while an open circle (○) represents a principal node, which is a carbon atom carrying three substitution positions.

planted promolecule) is represented by the $\mathbf{C}_{3v}$-skeleton (**46**) with a set of three alkyl ligands as proligands.

The three positions (1 to 3) of $\mathbf{C}_{3v}$-skeleton (**46**) construct an orbit governed by a CR $\mathbf{C}_{3v}(/\mathbf{C}_s)$. According to Theorem 19.7 of Fujita's book,[20] we obtain the corresponding PCI-CFs as follows:

$$\text{PCI-CF}(\mathbf{C}_1, \$_d) = \frac{1}{6}b_1^3 - \frac{1}{2}a_1^2c_2 - \frac{1}{6}b_3 + \frac{1}{2}a_3, \tag{44}$$

$$\text{PCI-CF}(\mathbf{C}_s, \$_d) = a_1c_2 - a_3 \tag{45}$$

$$\text{PCI-CF}(\mathbf{C}_3, \$_d) = \frac{1}{2}b_3 - \frac{1}{2}a_3, \tag{46}$$

$$\text{PCI-CF}(\mathbf{C}_{3v}, \$_d) = a_3, \tag{47}$$

where we use the USCI-CF table and the inverse table of marks for the isomorphic group $\mathbf{C}_{3v}$ (Appendices E.7 and B.7 of Fujita's book[20]).

By summing up the PCI-CFs shown in eqs. 44–47, we obtain the following CI-CF:

$$\text{CI-CF}(\mathbf{C}_{3v}; \$_d) = \frac{1}{6}b_1^3 + \frac{1}{2}a_1c_2 + \frac{1}{3}b_3 \tag{48}$$

By summing up eq. 45 and eq. 47, we obtain the following CI-CF$_A$ for counting achiral planted promolecules:

$$\begin{aligned} \text{CI-CF}_A(\mathbf{C}_{3v}; \$_d) &= \text{PCI-CF}(\mathbf{C}_s; \$_d) + \text{PCI-CF}(\mathbf{C}_{3v}; \$_d) \\ &= a_1c_2 \end{aligned} \tag{49}$$

The CI-CFs (eqs. 48 and 49) are identical with the ones derived by means of Fujita's proligand method,[26–28] although the SIs in eq. 36 are concerned with the sphericities of orbits of cycle subgroups, while the SIs in the CI-CF of Fujita's proligand method are concerned with the sphericities of cycles.

By the inspection of the ligand inventories shown in eqs. 17 and 39, the b_d is evaluated by using the following CI-CF:

$$\begin{aligned} \text{CI-CF}(\mathbf{C}_3; b_d) &= \text{PCI-CF}(\mathbf{C}_s; \$_d) + \text{PCI-CF}(\mathbf{C}_{3v}; \$_d) \\ &\quad + 2\text{PCI-CF}(\mathbf{C}_1; \$_d) + 2\text{PCI-CF}(\mathbf{C}_3; \$_d) \\ &= \frac{1}{3}b_1^3 + \frac{2}{3}b_3, \end{aligned} \tag{50}$$

which is identical with the CI-CF derived by means of Fujita's proligand method[26–28] for the $\mathbf{C}_3$-point group.

By the inspection of the ligand inventories shown in eqs. 16 and 38, the c_d is evaluated by counting diploids, although the detailed derivation is not described in this paper. We use the following CI-CF:

$$\text{CI-CF}_D(\mathbf{C}_3, c_{2d}) = \frac{1}{3}(c_2^3 + 2c_6). \tag{51}$$

The CI-CFs for the $\mathbf{C}_{3v}$-skeleton (eqs. 49–51) can be applied to recursive calculations of ligands of carbon content k. According to Fujita's proligand method,[26–28] they are transformed into the following functional equations:

$$a(x) = 1 + xa(x)c(x^2) \tag{52}$$

$$c(x^2) = 1 + \frac{x^2}{3}\left(c(x^2)^3 + 2c(x^6)\right) \tag{53}$$

$$b(x) = 1 + \frac{x}{3}\left(b(x)^3 + 2b(x^3)\right), \tag{54}$$

where the sphericity indices (a_d, c_d, and b_d) of the CI-CFs are replaced by $a(x^d)$, $c(x^d)$, and $b(x^d)$. For example, eq. 52 is obtained from eq. 49, where the term x is multiplied to take account of a principal node and the first constant term 1 is added to treat a null vertex (hydrogen atom). The functional equations (eqs. 52–54) have recursive nature so as to support the procedure described in Fig. 5.

4 Centroidal and Bicentroidal 3D-Trees

When alkanes are enumerated as 3D-trees, they are categorized into either centroidal 3D-trees or bicentroidal ones according to Jordan.[35] The centroidal 3D-trees are enumerated on the basis of the $\mathbf{T}_d$-skeleton (**1**), while the bicentroidal 3D-trees are enumerated on the basis of the **K**-skeleton (**39**).

Let us define a tree (or a 3D-tree) as a graph (or a 3D-object) which has v vertices and e edges satisfying the relation $v = e + 1$. Let m be the number of vertices contained in the largest branch among the branches attaching to the vertex. Trees (or 3D-trees) are classified into two categories, i.e., centroidal trees (or 3D-trees) and bicentroidal trees (or 3D-trees).[35]

1. A given tree (or 3D-tree) has an exceptional vertex (M) called a *centroid* if it satisfies the relationship $m < \frac{1}{2}v$. The tree (or 3D-tree) is called a *centroidal tree* (or *centroidal 3D-tree*).

2. A given tree (or 3D-tree) has two adjacent vertices (M_1 and M_2), each of which satisfies the relationship $m = \frac{1}{2}v$. The exceptional graph (M_1—M_2) composed of the two adjacent vertices and the relevant edge is called a *bicentroid*. The tree (or 3D-tree) is called a *bicentroidal tree* (or *bicentroidal 3D-tree*).

All of the vertices of the tree (or 3D-tree) other than the centroid or the bicentroid satisfy the relationship $m > \frac{1}{2}v$. There are no cases in which a given tree (or 3D-tree) has both a centroid and a bicentroid so that a kind of dichotomy takes place.

5 Alkanes as Centroidal 3D-Trees

5.1 Tetrahedral Promolecules into Centroidal Alkanes

Tetrahedral promolecules described in Subsection 2.1 are converted into centroidal alkanes, where the four proligands of each tetrahedral promolecule are replaced by alkyl ligands described in Section 3. For example, a promolecule **5** derived from the $\mathbf{T}_d$-skeleton **1** is in turn converted into 3,3-dimethylpentane (**49**) as a centroidal alkane of carbon content 7, where the proligands X and Y are replaced by a methyl (CH_3) and an ethyl ligand (CH_2CH_3) respectively, as shown in Fig. 6.

Because the promolecule **5** belongs to the $\mathbf{C}_{2v}$-point group (cf. Fig. 2), the 3,3-dimethylpentane is regarded as belonging to the $\mathbf{C}_{2v}$-point group as an average conformation. Strictly speaking, such assignment to point groups requires the concept of matching or mismatching for the relationships between promolecules and molecules.[29] For the sake of convenience and simplicity, however, we presume here that an alkane is characterized by the point group of the corresponding promolecule.

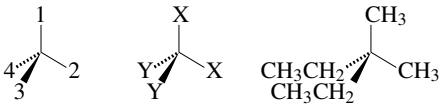

Figure 6: $\mathbf{T}_d$-skeleton (**1**) with four substitution positions, a tetrahedral promolecule (**5**), and a centroidal alkane (**49**).

Alkyl ligands, which are enumerated by the generating functions regarded as ligand inventories (eqs. 41–43), are introduced into the promolecule (**5**) under the criterion of centroidal 3D-trees (Section 4). When such alkyl ligands have been counted up to carbon content $m = 3$, for example, the numbers of alkanes of carbon content 7 or 8 ($2m+1 = 7$ and $2m + 2 = 8$) can be evaluated. As for the term x^7 of the carbon content 7, the following modes of factorization take place: $x^3 \cdot x^3 \cdot x^0 \cdot x^0 \times x$ for heptane (two hydrogens and two *n*-propyl ligands, **5**, $\mathbf{C}_{2v}$), 2-methylhexane (two hydrogens and a *n*-propyl and an isopropyl, **11**, $\mathbf{C}_s$), and 2,4-dimethylpentane (two hydrogens and two isopropyl ligands, **5**, $\mathbf{C}_{2v}$); $x^3 \cdot x^2 \cdot x^1 \cdot x^0 \times x$ for 3-methylhexane (a hydrogen, a methyl, an ethyl, and a *n*-propyl, **19**, $\mathbf{C}_1$) and for 2,3-methylpentane (a hydrogen, a methyl, an ethyl, and an isopropyl, **19**, $\mathbf{C}_1$); $x^3 \cdot x^1 \cdot x^1 \cdot x^1 \times x$ for 2,2-dimethylpentane (three methyls and a *n*-propyl, **4**, $\mathbf{C}_{3v}$) and 2,2,3-trimethylbutane (three methyls and an isopropyl, **4**, $\mathbf{C}_{3v}$); $x^2 \cdot x^2 \cdot x^2 \cdot x^0 \times x$ for 3-ethylpentane (three ethyl ligands, **4**, $\mathbf{C}_{3v}$); as well as $x^2 \cdot x^2 \cdot x^1 \cdot x^1 \times x$ for 3,3-dimethylpentane (**49**, $\mathbf{C}_{2v}$). Note that the power of each factorized term should be equal to or less than $m = 3$. Hence, all of the possible modes of factorization for $v = 7$ appear in this enumeration under the criterion of centroidal 3D-trees ($m < (1/2)v = 7/2$). Other modes of factorization, e.g., $x^4 \cdot x^2 \cdot x^0 \cdot x^0 \times x$ for heptane, do not appear.

The procedure described in the preceding paragraph is extended to cover general cases,

as described in the following subsections.

5.2 Functional Equations for Counting Centroidal 3D-Trees

Let **H** be a subgroup of the $\mathbf{T}_d$-point group. Let $N_k^{(\mathbf{H})}$ be the number of centroidal alkanes (or 3D-trees) which belong to **H** and have carbon content k. Throughout the enumerations described in this paper, each pair of enantiomeric 3D-trees is counted just once. In agreement with the definition of centroidal 3D-trees, the terms up to x^v are collected to give the following generating functions:

$$N(x)^{(\mathbf{H})} = \sum_{k=0}^{v} N_k^{(\mathbf{H})} x^k \tag{55}$$

where v runs stepwise from 0 to infinite. Because each of eqs. 2–12 corresponds to eq. 55, the SIs a_d, c_d, and b_d are replaced by the terms $a(x^d)$, $c(x^d)$, and $b(x^d)$ respectively. Thereby we obtain the following functional equations:

$$\begin{aligned}
N(x)^{(\mathbf{C}_1)} &= \frac{1}{24}b(x)^4 - \frac{1}{8}b(x^2)^2 - \frac{1}{4}a(x)^2c(x^2) - \frac{1}{6}b(x)b(x^3) \\
&\quad + \frac{1}{12}b(x^4) + \frac{1}{4}a(x^2)^2 + \frac{1}{2}a(x)a(x^3) + \frac{1}{6}b(x^4) - \frac{1}{2}a(x^4) && (56)\\
N(x)^{(\mathbf{C}_2)} &= \frac{1}{4}b(x^2)^2 - \frac{1}{4}c(x^4) - \frac{1}{4}b(x^4) - \frac{1}{4}a(x^2)^2 + \frac{1}{2}a(x^4) && (57)\\
N(x)^{(\mathbf{C}_s)} &= \frac{1}{2}a(x)^2c(x^2) - \frac{1}{2}a(x^2)^2 - a(x)a(x^3) + a(x^4) && (58)\\
N(x)^{(\mathbf{C}_3)} &= \frac{1}{2}b(x)b(x^3) - \frac{1}{2}a(x)a(x^3) - \frac{1}{2}b(x^4) + \frac{1}{2}a(x^4) && (59)\\
N(x)^{(\mathbf{S}_4)} &= \frac{1}{2}c(x^4) - \frac{1}{2}a(x^4) && (60)\\
N(x)^{(\mathbf{D}_2)} &= 0 && (61)\\
N(x)^{(\mathbf{C}_{2v})} &= \frac{1}{2}a(x^2)^2 - \frac{1}{2}a(x^4) && (62)\\
N(x)^{(\mathbf{C}_{3v})} &= a(x)a(x^3) - a(x^4) && (63)\\
N(x)^{(\mathbf{D}_{2d})} &= 0 && (64)\\
N(x)^{(\mathbf{T})} &= \frac{1}{2}b(x^4) - \frac{1}{2}a(x^4) && (65)\\
N(x)^{(\mathbf{T}_d)} &= a(x^4), && (66)
\end{aligned}$$

Our target is to evaluate $N(x)^{(\mathbf{H})}$ (eqs. 56–66) by using eqs. 52–54 under the criterion for centroidal 3D-trees. The criterion for centroidal 3D-trees means that the maximum number (m), which is the number of non-terminal vertices in the largest proligand, is restricted to satisfy the following condition:

$$\frac{1}{2}v - 1 \le m < \frac{1}{2}v \tag{67}$$

or equivalently

$$2m < v \le 2m + 2, \tag{68}$$

because the number m moves stepwise during the recursive calculation.

Suppose that eqs. 52–54 have been evaluated up to the term x^m. That is to say, we have obtained the generating functions, i.e., $a(x) = \sum_{k=0}^{m} \alpha_k x^k$, $c(x^2) = \sum_{k=0}^{m} \gamma_k x^{2k}$, and $b(x) = \sum_{k=0}^{m} \beta_k x^k$, where m is tentatively fixed. They are introduced into the right-hand sides of eqs. 56–66 and the resulting equations are expanded to give respective series $N(x)^{(\mathbf{H},m)}$, each of which is used to give the coefficients of eq. 55. Because of eq. 68, the coefficients of the terms x^{2m+1} and x^{2m+2} in the series are effective to determine $N_{2m+1}^{(\mathbf{H})}$ and $N_{2m+2}^{(\mathbf{H})}$. Let the symbol coeff$(N(x)^{(\mathbf{H},m)}, x^{2m+1})$ etc. represent the coefficient of the term x^{2m+1} appearing in the equation $N(x)^{(\mathbf{H},m)}$ etc. after expansion. Then, we obtain the following coefficients:

$$N_{2m+1}^{(\mathbf{H})} = \text{coeff}(N(x)^{(\mathbf{H},m)}, x^{2m+1}) \tag{69}$$

for odd carbon contents as well as the following coefficients:

$$N_{2m+2}^{(\mathbf{H})} = \text{coeff}(N(x)^{(\mathbf{H},m)}, x^{2m+2}) \tag{70}$$

for even carbon contents. These requirements should be considered in the following programming.

5.3 Achiral Centroidal Alkanes

By using the Maple programming language,[36] we wrote a program for evaluating $a(x)$, $c(x^2)$, and $b(x)$ (eqs. 52–54) and for obtaining the coefficients $N_k^{(\mathbf{H})}$ (eq. 55), where the functional equations for achiral subgroups, i.e., $\mathbf{C}_s$ (eq. 58), $\mathbf{S}_4$ (eq. 60), $\mathbf{C}_{2v}$ (eq. 62), $\mathbf{C}_{3v}$ (eq. 63), $\mathbf{D}_{2d}$ (eq. 64), and $\mathbf{T}_d$ (eq. 66), are selected. The program was stored in a file named "CentrSIA1-100.mpl", which was executed by inputting as follows:

```
read "CentrSIA1-100.mpl";
```

on a display window of the Maple system. The results are shown in Table 1, where the values of $N_k^{(\mathbf{H})}$ for achiral centroidal 3D-trees, are collected up to carbon content $k = 100$.

Maple program for counting achiral centroidal 3D-trees, "CentrSIA1-100.mpl":

```
"Functional Equations for Alkyl Ligands";
ax := 1 + x*a1*c2;
cx := 1+ (1/3)*x^2*c2^3 + (2/3)*x^2*c6;
bx := 1 + (1/3)*x*b1^3 + (2/3)*x*b3;

"Achiral Alkanes as Centroidal 3D-Trees";
NxCs := (x/2)*a1^2*c2 - (x/2)*a2^2 - x*a1*a3 + x*a4:
NxS4 := (x/2)*c4 - (x/2)*a4:
NxC2v := (x/2)*a2^2 - (x/2)*a4:
NxC3v := x*a1*a3 - x*a4:
NxD2d := 0:
NxTd := x*a4:

"Initial Values";
a1 := 1; a2 := 1; a3 := 1; a4 := 1;
b1 := 1; b2 := 1; b3 := 1; b4 := 1;
c2 := 1; c4 := 1; c6 := 1;
NCs := 0; NS4 := 0; NC2v := 0; NC3v := 0;
```

```
ND2d := 0; NTd := x;

"Recursive Calculation";
for m from 1 to 50 by 1 do
m:
Cbx:= coeff(bx,x^m):
Cax:= coeff(ax,x^m):
Ccx:= coeff(cx,x^(m*2)):
a1 := a1 + Cax*x^m:
a2 := a2 + Cax*x^(m*2):
a3 := a3 + Cax*x^(m*3):
a4 := a4 + Cax*x^(m*4):
b1 := b1 + Cbx*x^m:
b2 := b2 + Cbx*x^(m*2):
b3 := b3 +Cbx*x^(m*3):
b4 := b4 +Cbx*x^(m*4):
c2 := c2 + Ccx*x^(m*2):
c4 := c4 + Ccx*x^(m*4):
c6 := c6 + Ccx*x^(m*6):
n := 2*m +1:
NCs := NCs + coeff(NxCs,x^n)*x^n + coeff(NxCs,x^(n+1))*x^(n+1):
NS4 := NS4 + coeff(NxS4,x^n)*x^n + coeff(NxS4,x^(n+1))*x^(n+1):
NC2v := NC2v + coeff(NxC2v,x^n)*x^n + coeff(NxC2v,x^(n+1))*x^(n+1):
NC3v := NC3v + coeff(NxC3v,x^n)*x^n + coeff(NxC3v,x^(n+1))*x^(n+1):
# ND2d := 0:
NTd := NTd + coeff(NxTd,x^n)*x^n + coeff(NTd,x^(n+1))*x^(n+1):
end do:

"Print-Out";
for m from 1 to 100 by 1 do
printf("%d & %d & %d & %d & %d & %d & %d \\\\ \n",
m, coeff(NCs,x^m), coeff(NS4,x^m), coeff(NC2v,x^m),
coeff(NC3v,x^m), coeff(ND2d,x^m), coeff(NTd,x^m));
end do;
```

In this program, the first paragraph "Functional Equations for Alkyl Ligands" declares the functional equations for calculating $a(x)$ (`ax`), $c(x^2)$ (`cx`), and $b(x)$ (`bx`). The second paragraph "Achiral Alkanes as Centroidal 3D-Trees" describes the functional equations for calculating $N(x)^{(\mathbf{C}_s)}$ (`NxCs`), $N(x)^{(\mathbf{S}_4)}$ (`NxS4`), $N(x)^{(\mathbf{C}_{2v})}$ (`NxC2v`), $N(x)^{(\mathbf{C}_{3v})}$ (`NxC3v`), $N(x)^{(\mathbf{D}_{2d})}$ (`NxD2d`), and $N(x)^{(\mathbf{T}_d)}$ (`NxTd`). The third paragraph "Initial Values" gives the initial values for every functional equations. Note that the initial value for $N(x)^{(\mathbf{T}_d)}$ is equal to x because methane (CH_4) belongs to the $\mathbf{T}_d$-point group. The initial values for the other subsymmetries are equal to 0. The fourth paragraph "Recursive Calculation" is composed of a `do` loop for recursive calculations, which are referred to by the symbol $N(x)^{(\mathbf{H},m)}$ in the text (cf. eqs. 69 and 70). The resulting values at each step of m are stored as the series denoted by the symbols `NCs`, `NS4`, and so on. Because the value for `ND2d` is always equal to zero, its calculation is comment out by the top symbol `#`. Note that m moves from 1 to 50 to calculate the values `NCs`, `NS4`, etc. up to carbon content 100. The last paragraph "Print-Out" declares a `do` loop for printing out the values in a tabular form up to carbon content 100.

Table 1: Numbers of Achiral Centroidal Alkanes as Stereoisomers

k	$N_k^{(\mathbf{C}_s)}$	$N_k^{(\mathbf{S}_4)}$	$N_k^{(\mathbf{C}_{2v})}$	$N_k^{(\mathbf{C}_{3v})}$	$N_k^{(\mathbf{D}_{2d})}$	$N_k^{(\mathbf{T}_d)}$
1	0	0	0	0	0	1
2	0	0	0	0	0	0
3	0	0	1	0	0	0
4	0	0	0	1	0	0
5	1	0	1	0	0	1
6	1	0	0	1	0	0
7	1	0	3	3	0	0
8	6	0	0	1	0	0
9	15	0	5	0	0	1
10	18	0	0	4	0	0
11	46	0	10	5	0	0
12	65	0	0	7	0	0
13	154	0	17	13	0	2
14	211	0	0	9	0	0
15	521	0	33	13	0	0
16	690	0	0	27	0	0
17	1654	1	58	39	0	3
18	2143	0	0	66	0	0
19	5221	0	109	124	0	0
20	7084	0	0	65	0	0
21	16770	3	195	97	0	5
22	22283	0	0	193	0	0
23	52953	0	360	315	0	0
24	72121	0	0	535	0	0
25	167573	10	648	936	0	8
26	229154	0	0	522	0	0
27	533192	0	1188	887	0	0
28	741459	0	0	1567	0	0
29	1693439	30	2145	2694	0	14
30	2356842	0	0	4634	0	0
31	5388748	0	3917	8243	0	0
32	7638453	0	0	4440	0	0
33	17196595	88	7086	7576	0	23
34	24381264	0	0	13515	0	0
35	54910864	0	12909	23374	0	0
36	78968566	0	0	41160	0	0
37	175606614	255	23372	72096	0	41
38	252924049	0	0	40361	0	0
39	562532305	0	42527	71105	0	0
40	819797708	0	0	124587	0	0
41	1803790125	742	77035	220425	0	69
42	2631434593	0	0	386151	0	0
43	5790670695	0	140056	686971	0	0
44	8536007187	0	0	369973	0	0
45	18610917131	2157	253773	647978	0	122
46	27457004166	0	0	1152542	0	0
47	59867785527	0	461144	2026617	0	0
48	89117135300	0	0	3605944	0	0
49	192755488759	6312	835700	6363261	0	208
50	287163973973	0	0	3562173	0	0
51	621137200090	0	1518054	6339866	0	0
52	932625463618	0	0	11186006	0	0
53	2003037478871	18563	2751329	19944650	0	370
54	3009690158892	0	0	35253548	0	0
55	6463933786931	0	4996532	62963143	0	0
56	9780002561496	0	0	33997046	0	0
57	20873352533838	54932	9056320	60098723	0	636
58	31600801024417	0	0	107317305	0	0
59	67444985008482	0	16443444	190086714	0	0
60	102742981680520	0	0	339779060	0	0
61	218049270634929	163479	29805337	602876800	0	1134
62	332349944192206	0	0	333426006	0	0
63	705329515771177	0	54108871	596072824	0	0
64	1081085992129251	0	0	1057517930	0	0
65	2282684405651049	489264	98080592	1892473149	0	1963
66	3500475452272016	0	0	3362138313	0	0
67	7391010089853174	0	178033983	6022079973	0	0
68	11391630773729656	0	0	9261038354	0	0
69	23941651849179155	1471692	322721226	57940993631	0	3505
70	36917151200853395	0	0	103767271195	0	0
71	77586362420289576	0	585735965	184600094006	0	0
72	120189276606249019	0	0	330850451997	0	0
73	251528875360291015	4447896	1061779881	589227819020	0	6099
74	389800749815698542	0	0	825839784590	0	0
75	815741080006783242	0	1926948562	2584043364230	0	0
76	1269537821984296021	0	0	4040070551350	0	0
77	2646489706243291717	13500689	3493085670	12654970025010	0	10908
78	4120240650615704467	0	0	39253342384100	0	0
79	8588823952551671478	0	6338864653	123679600349100	0	0
80	13423903249778712026	0	0	323606786081000	0	0
81	27882747868810955737	41140608	11490954322	1012768722113600	0	19059
82	43593967477275496712	0	0	3203524231951950	0	0
83	90545954304171412196	0	20851110653	6487118737549000	0	0
84	142077347785803068205	0	0	10164833868860000	0	0
85	294122269463933345989	125818217	37798845063	31922058010954000	0	34129
86	461655250191909536942	0	0	100327133940518600	0	0
87	955666443324898385416	0	68584499782	314740575100230000	0	0
88	1505041724743622281946	0	0	988837232776800000	0	0
89	3105981780141689407555	386050543	124331000890	19842063804323000000	0	59836
90	4892884009202894931687	0	0	62667334055633000000	0	0
91	10097190645589970892216	0	225581833688	197284606610896000000	0	0
92	15955816346995486825756	0	0	622677807416000000000	0	0
93	32832697521558748114222	1188093392	408941516928	1961599693177400000000	0	107256
94	51896703487573652186666	0	0	6181497890299900000000	0	0
95	106785552550444794979279	0	741934546674	19486299752858860000000	0	0
96	169281344122751160088724	0	0	61430728623633400000000	0	0
97	347387514775525048819112	3666547089	1345011197752	193766070237456640000000	0	188576
98	550829850998112137146017	0	0	1737217227407700000000000	0	0
99	1130336589786928318017011	0	2440124982590	5485178433957670000000000	0	0
100	1797192676445358205539276	0	0	17316351779527740000000000	0	0

5.4 Chiral Centroidal Alkanes

On a similar line, we wrote a program for evaluating the coefficients $N_k^{(\mathbf{H})}$ (eq. 55), where $\mathbf{H}$ covers chiral subgroups, i.e., $\mathbf{C}_1$ (eq. 56), $\mathbf{C}_2$ (eq. 57), $\mathbf{C}_3$ (eq. 59), $\mathbf{D}_2$ (eq. 61), and $\mathbf{T}$ (eq. 65). The program was stored in a file named "CentrSIC1-100.mpl", which was executed on a display window of the Maple system. The results are shown in Table 2, where the values of $N_k^{(\mathbf{H})}$ for chiral centroidal alkanes as 3D-trees are collected up to carbon content $k = 100$.

Maple program for counting achiral centroidal 3D-trees, "CentrSIC1-100.mpl":

```
"Functional Equaitons for Alkyl Ligands";
ax := 1 + x*a1*c2;
cx := 1+ (1/3)*x^2*c2^3 + (2/3)*x^2*c6;
bx := 1 + (1/3)*x*b1^3 + (2/3)*x*b3;

"Chiral Alkanes as Centroidal 3D-Trees";
NxC1 := (x/24)*b1^4 - (x/8)*b2^2 - (x/4)*a1^2*c2 - (x/6)*b1*b3
+ (x/12)*b4 + (x/4)*a2^2 + (x/2)*a1*a3 + (x/6)*b4 - (x/2)*a4:
NxC2 := (x/4)*b2^2 - (x/4)*c4 -(x/4)*b4 - (x/4)*a2^2 + (x/2)*a4:
NxC3 := (x/2)*b1*b3 - (x/2)*a1*a3 - (x/2)*b4 + (x/2)*a4:
NxD2 := 0:
NxT := (x/2)*b4 - (x/2)*a4:

"Initial Values";
a1 := 1; a2 := 1; a3 := 1; a4 := 1;
b1 := 1; b2 := 1; b3 := 1; b4 := 1;
c2 := 1; c4 := 1; c6 := 1;

NC1 := 0; NC2 := 0; NC3 := 0;
ND2 := 0; NT := 0;

"Recursive Calculation";
for m from 1 to 50 by 1 do
m:
Cbx:= coeff(bx,x^m):
Cax:= coeff(ax,x^m):
Ccx:= coeff(cx,x^(m*2)):
a1 := a1 + Cax*x^m:
a2 := a2 + Cax*x^(m*2):
a3 := a3 + Cax*x^(m*3):
a4 := a4 + Cax*x^(m*4):
b1 := b1 + Cbx*x^m:
b2 := b2 + Cbx*x^(m*2):
b3 := b3 +Cbx*x^(m*3):
b4 := b4 +Cbx*x^(m*4):
c2 := c2 + Ccx*x^(m*2):
c4 := c4 + Ccx*x^(m*4):
c6 := c6 + Ccx*x^(m*6):
n := 2*m +1:
NC1 := NC1 + coeff(NxC1,x^n)*x^n + coeff(NxC1,x^(n+1))*x^(n+1):
NC2 := NC2 + coeff(NxC2,x^n)*x^n + coeff(NxC2,x^(n+1))*x^(n+1):
NC3 := NC3 + coeff(NxC3,x^n)*x^n + coeff(NxC3,x^(n+1))*x^(n+1):
#ND2 := 0
NT := NT + coeff(NxT,x^n)*x^n + coeff(NT,x^(n+1))*x^(n+1):
end do:
```

Table 2: Numbers of Chiral Centroidal Alkanes as Stereoisomers

k	$N_k^{(\mathbf{C}_1)}$	$N_k^{(\mathbf{C}_2)}$	$N_k^{(\mathbf{C}_3)}$	$N_k^{(\mathbf{D}_2)}$	$N_k^{(\mathbf{T})}$
1	0	0	0	0	0
2	0	0	0	0	0
3	0	0	0	0	0
4	0	0	0	0	0
5	0	0	0	0	0
6	0	0	0	0	0
7	2	0	0	0	0
8	1	0	0	0	0
9	16	1	0	0	0
10	24	0	0	0	0
11	137	4	1	0	0
12	208	0	3	0	0
13	1088	14	11	0	0
14	1781	0	3	0	0
15	8728	45	7	0	0
16	15016	0	25	0	0
17	70542	137	70	0	1
18	126873	0	199	0	0
19	583161	413	584	0	0
20	1091313	0	194	0	0
21	4935871	1224	518	0	3
22	9552669	0	1500	0	0
23	42610014	3628	4239	0	0
24	84913438	0	12108	0	0
25	374534342	10726	35194	0	10
26	765726198	0	9601	0	0
27	3344120073	31849	27247	0	0
28	6991607622	0	79017	0	0
29	30262097640	94812	230097	0	30
30	64535064481	0	676270	0	0
31	277089116563	283626	2004533	0	0
32	601433497064	0	589702	0	0
33	2563398497146	851908	1730852	0	88
34	5652870902224	0	5127624	0	0
35	23930979266113	2570487	15283550	0	0
36	53534778745686	0	45831332	0	0
37	225225704062298	7787458	138190733	0	255
38	510446235179592	0	40491657	0	0
39	2135108531527988	23686702	121401546	0	0
40	4896888481848366	0	366009579	0	0
41	20372873595205767	72306778	1108653460	0	742
42	47238608059106749	0	3372550565	0	0
43	195544777082357941	221475758	10299053406	0	0
44	457999548956981900	0	2990846713	0	0
45	1886989250713218801	680486457	9097599635	0	2157
46	4461040341712135844	0	27780675238	0	0
47	18298681595332091514	2096823118	85127192309	0	0
48	43636081193349667700	0	261679492103	0	0
49	178246301608070153586	6478177469	806728738098	0	6312
50	428497964650142021424	0	236153410997	0	0
51	1743475976503183715969	20063555673	725913625056	0	0
52	4222957576043374182661	0	2237863494713	0	0
53	17118606491555519010253	62279760278	6917251510288	0	18563
54	41757572996188827520560	0	21433502624921	0	0
55	168676827104237821826538	193731258600	66562691413856	0	0
56	414192406671150318072106	0	19524289580960	0	0
57	1667507044024423133622455	603812096114	60496333096712	0	54932
58	4120269448840606530096592	0	187871793480876	0	0
59	16535111534667814115851179	1885366277126	584655745189860	0	0
60	41098222464201188479721461	0	1822973727951104	0	0
61	164431690998772629953765002	5896973066736	5694351363421114	0	163479
62	410979018220114666421210927	0	1672219254165487	0	0
63	1639544206282824773990638754	18473739020239	5213980357641853	0	0
64	4119529788239166095158905426	0	16286567011875508	0	0
65	16388819934840328046163962344	57960178877629	50959078719141813	0	489264
66	41385225782086638716982598146	0	159697603469199852	0	0
67	164207682036340696679355917760	182102032083179	501207333060096255	0	0
68	416635607643425685493790619639	0	147564316141568856	0	0
69	1648923729893500748643868730611	572894057771620	462440219463967987	0	1471692
70	4202708638019194596613346990021	0	1451350204852807945	0	0
71	16592589875608595359992019209976	1804577898019896	4561339961810127869	0	0
72	42473372537677850472777542629383	0	14354263936717538576	0	0
73	167295424464158756775720063838179	5691002482822708	45227789621187113168	0	4447896
74	430006772381297681343212302777548	0	13340319433398214532	0	0
75	1689911835064521935507132475924052	17967439710311488	41981014458194046088	0	0
76	4360786726830706504336113212213232	0	132274367651117787152	0	0
77	17100609751073724255686898881677495	56786161588395299	417258211604024603398	0	13500689
78	44294354185220865010398773718204079	0	1317690129367286189362	0	0
79	173335468778159593163913331435064754	179652924061845438	4165583177663598506736	0	0
80	450600427378155601531524267538618101	0	1230604554959778468323	0	0
81	1759767313496474041294340569031428476	568905113680499543	3886204142045452877624	0	41140608
82	4590528948690459275690584150945517385	0	12285331976808314853923	0	0
83	17892924987803287856662098419745700484	1803179865827956647	38875788611736411229781	0	0
84	46830869858741035982999884879739090944	0	123134889567482431417299	0	0
85	182194157793655314127689578349954352057	5720226829686477505	390366705393287456688781	0	125818217
86	478379522345454563342723736582044188225	0	115505492526757165241910	0	0
87	1857742280338673100733168084362718159515	18161221880947045354	365850446898209994701499	0	0
88	4892807796459915367926695352825895331513	0	1159829967559571185462075	0	0
89	18967377099179000185734335092653847026113	57705644326488454668	3680072615060589057215203	0	386050543
90	50103146420285102048745073165752201512985	0	11686180909071862117268062	0	0
91	193898555422930409852147554822891928264315	183492290401870276634	37138723437443860483678486	0	0
92	513654043751710283713518927751179291782910	0	11004204547923141886912994	0	0
93	1984557489015003195976562360507756970203368	583887944881163008868	34944123148744982244286724	0	1188093392
94	5271743914770706146908560703076785683941544	0	111052368499755401970352795	0	0
95	20335387509472989845379192184310377893539742	1859259968236169909768	353187028940557839273753415	0	0
96	54162175051500718278191209798478444849365395	0	1124063728478422617779311600	0	0
97	208602785663318652002726980250253244278651001	5924302673970710021581	3579919884736380393562521144	0	3666547089
98	557028727906484284276879203374610568962096776	0	1062063691969548850469476432	0	0
99	2142136450298921144580392613201845315725938448	18889010758760410834979	3380151703727978578140353524	0	0
100	5734313151200075256443744285442491428332933296	0	10765099115434986558331481893	0	0

```
"Print-Out";
for m from 1 to 100 by 1 do
printf("%d & %d & %d & %d & %d & %d  \\\\ \n",
m, coeff(NC1,x^m), coeff(NC2,x^m), coeff(NC3,x^m),
coeff(ND2,x^m), coeff(NT,x^m));
end do;
```

The program "CentrSIC1-100.mpl" essentially has the same constitution as the program named "CentrSIA1-100.mpl" except that it is concerned with the functional equations for chiral centroidal 3D-trees: $\mathbf{C}_1$ (eq. 56), $\mathbf{C}_2$ (eq. 57), $\mathbf{C}_3$ (eq. 59), $\mathbf{D}_2$ (eq. 61), and $\mathbf{T}$ (eq. 65). The resulting values at each step of m, which is referred to by the symbol $N(x)^{(\mathbf{H},m)}$ in the text (cf. eqs. 69 and 70), are stored as the series denoted by the symbols `NC1`, `NC2`, and so on. Because the value for `ND2` is always equal to zero, its calculation is comment out by the top symbol `#`. Note again that m moves from 1 to 50 to calculate the values `NC1`, `NC2`, etc. up to carbon content 100. The last paragraph "Print-Out" declares a `do` loop for printing out the values in a tabular form up to carbon content 100.

5.5 Total Numbers of Achiral and Chiral Centroidal Alkanes

Table 1 and 2 give the symmetry-itemized numbers of centroidal alkanes. Total numbers without such symmetry-itemization are sometimes convenient to grasp total features of alkanes. Let $\widehat{B}_k$, $\widehat{A}_k$, and $\widehat{C}_k$ be the number of achiral and chiral centroidal alkanes, the number of achiral centroidal alkanes, and the number of chiral centroidal alkanes, respectively, where the subscript k represents a carbon content and a pair of enantiomeric alkanes is counted just once. In agreement with the definition of centroidal 3D-trees, the terms up to x^v are collected to give the following generating functions:

$$\widehat{B}(x) = \sum_{k=0}^{v} \widehat{B}_k x^k \tag{71}$$

$$\widehat{A}(x) = \sum_{k=0}^{v} \widehat{A}_k x^k \tag{72}$$

$$\widehat{C}(x) = \sum_{k=0}^{v} \widehat{C}_k x^k, \tag{73}$$

where v runs stepwise from 0 to infinite. These equations are compared with eq. 55 to give the following relationships:

$$\widehat{B}_k = \sum_{\text{all } \mathbf{H}} N_k^{(\mathbf{H})} \tag{74}$$

$$\widehat{A}_k = \sum_{\text{achiral } \mathbf{H}} N_k^{(\mathbf{H})} \tag{75}$$

$$\widehat{C}_k = \sum_{\text{chiral } \mathbf{H}} N_k^{(\mathbf{H})}. \tag{76}$$

Because each $N_k^{(\mathbf{H})}$ in the right-hand sides of eqs. 74–76 have been calculated in the preceding subsections, eqs. 74–76 can be evaluated easily by the summation of relevant values. For example, eq. 75 is evaluated by summing up of each row of Table 1 and eq.

76 is evaluated by summing up of each row of Table 2. These summation procedures can be conducted by merging the programs "CentrSIA1-100.mpl" and "CentrSIC1-100.mpl" and adding such lines as follows:

```
TotalB := NC1 + NC2 + NCs + NC3 + NS4 + NC2v + NC3v + NT + NTd:
TotalA := NCs + NS4 + NC2v + NC3v + NTd:
TotalC := NC1 + NC2 + NC3 + NT:

"Print-Out";
for m from 1 to 100 by 1 do
printf("%d & %d & %d & %d \\\\ \n",
m, coeff(TotalA,x^m), coeff(TotalC,x^m), coeff(TotalB,x^m));
end do;
```

The symbols `TotalB`, `TotalA`, and `TotalC` represent eqs. 74–76. The resulting program was executed to give Table 3.

To evaluate eqs. 74–76 directly, respective CI-CFs are obtained by starting from the PCI-CFs listed in eqs. 2–12. First, the PCI-CFs for achiral proligands are selected from eqs. 2–12 and they are summed up to give following CI-CF$_A$ for counting achiral tetrahedral promolecules:

$$\begin{aligned} \text{CI-CF}_A(\mathbf{T}_d, \$_d) &= \text{PCI-CF}(\mathbf{C}_s, \$_d) + \text{PCI-CF}(\mathbf{S}_4, \$_d) + \text{PCI-CF}(\mathbf{C}_{2v}, \$_d) \\ &\quad + \text{PCI-CF}(\mathbf{C}_{3v}, \$_d) + \text{PCI-CF}(\mathbf{D}_{2d}, \$_d) + \text{PCI-CF}(\mathbf{T}_d, \$_d) \\ &= \frac{1}{2}a_1^2 c_2 + \frac{1}{2}c_4. \end{aligned} \tag{77}$$

On a similar line, the PCI-CFs for chiral proligands are selected from eqs. 2–12 and they are summed up to give following CI-CF$_C$ for counting achiral tetrahedral promolecules:

$$\begin{aligned} \text{CI-CF}_C(\mathbf{T}_d, \$_d) &= \text{PCI-CF}(\mathbf{C}_1, \$_d) + \text{PCI-CF}(\mathbf{C}_2, \$_d) + \text{PCI-CF}(\mathbf{C}_3, \$_d) \\ &\quad + \text{PCI-CF}(\mathbf{D}_2, \$_d) + \text{PCI-CF}(\mathbf{T}, \$_d) \\ &= \frac{1}{24}b_1^4 + \frac{1}{8}b_2^2 + \frac{1}{3}b_1 b_3 - \frac{1}{4}a_1^2 c_2 - \frac{1}{4}c_4. \end{aligned} \tag{78}$$

By the summation of CI-CF$_A(\mathbf{T}_d, \$_d)$ (eq. 77) and CI-CF$_C(\mathbf{T}_d, \$_d)$ (eq. 78), we are able to obtain CI-CF$(\mathbf{T}_d, \$_d)$ (eq. 13) for counting achiral and chiral promolecules.

Because the generating functions shown in eq. 71, 72, and 73 correspond to CI-CFs shown in eqs. 13, 77, and 78, the SIs a_d, c_d, and b_d involved in the CI-CFs are replaced by the terms $a(x^d)$, $c(x^d)$, and $b(x^d)$ respectively. Thereby we obtain the following functional equations:

$$\widehat{B}(x) = \frac{x}{24}\{b(x)^4 + 3b(x^2)^2 + 8b(x)b(x^3) + 6a(x)^2 c(x^2) + 6c(x^4)\} \tag{79}$$

$$\widehat{A}(x) = \frac{x}{2}\{a(x)^2 c(x^2) + c(x^4)\} \tag{80}$$

$$\widehat{C}(x) = \frac{x}{24}\{b(x)^4 + 3b(x^2)^2 + 8b(x)b(x^3) - 6a(x)^2 c(x^2) - 6c(x^4)\}, \tag{81}$$

where the multiplying by x is necessary because of considering the centroid of the $\mathbf{T}_d$ skeleton. These equations are alternatively obtained by following Fujita's proligand method.[26–28]

Table 3: Numbers of Centroidal Alkanes as Stereoisomers

k	$\widehat{A}_k$ (Achiral)	$\widehat{C}_k$ (Chiral)	$\widehat{B}_k$ (Total)
1	1	0	1
2	0	0	0
3	1	0	1
4	1	0	1
5	3	0	3
6	2	0	2
7	7	2	9
8	7	1	8
9	21	17	38
10	22	24	46
11	61	142	203
12	72	211	283
13	186	1113	1299
14	220	1784	2004
15	567	8780	9347
16	717	15041	15758
17	1755	70750	72505
18	2209	127072	129281
19	5454	584158	589612
20	7149	1091507	1098656
21	17070	4937616	4954686
22	22476	9554169	9576645
23	53628	42617881	42671509
24	72656	84925546	84998202
25	169175	374580272	374749447
26	229676	765735799	765965475
27	535267	3344179169	3344714436
28	743026	6991686639	6992429665
29	1698322	30262422579	30264120901
30	2361476	64535740751	64538102227
31	5400908	277091404722	277096805630
32	7642893	601434086766	601441729659
33	17211368	2563401079994	2563418291362
34	24394779	5652876029848	5652900424627
35	54947147	23930997120150	23931052067297
36	79009726	53534824577018	53534903586744
37	175702378	225225850040744	225226025743122
38	252964410	510446275671249	510446528635659
39	562645937	2135108676616236	2135109239262173
40	819922295	4896888847857945	4896889667780240
41	1804088396	20372874776166747	20372876580255143
42	2631820744	47238611431657314	47238614063478058
43	5791497722	195544787602887105	195544793394384827
44	8536377160	457999551947828613	457999560484205773
45	18611821161	1886989260491307050	1886989279103128211
46	27458156708	4461040369492811082	4461040396950967790
47	59870273288	18298681682556106941	18298681742426380229
48	89120741244	43636081455029159803	43636081544149901047
49	192762694240	178246302421277075465	178246302614039769705
50	287167536146	428497964886295432421	428497965173462968567
51	621145058010	1743475977249160896698	1743475977870305954708
52	932636649624	4222957578281237677374	4222957579213874326998
53	2003060193783	17118606498535050299382	17118606500538110493165
54	3009644412440	41757573017622330145481	41757573020631974557921
55	6464001746606	168676827170994244498994	168676827177458246245600
56	9780036558542	414192406690674607653066	414192406700454644211608
57	20873421744449	1667507044085523278870213	1667507044106396700614662
58	31600908341722	4120269449028478323577468	4120269449060079231919190
59	67445191538640	16535111535254355227318165	16535111535321800418856805
60	102743321459580	41098222466024162207672565	41098222466126905529132145
61	218049903481679	164431691004472878290416331	164431691004690928193898010
62	332350277618212	410979018221786885675376414	410979018222119235952994626
63	705330165952872	1639544206288057228087300846	1639544206288762558253253718
64	1081087049647181	4119529788255452662170780934	4119529788256533749220428115
65	2282686396696017	16388819934891345085062471050	16388819934893627771459167067
66	3500478814410329	41385225782246336320451797998	41385225782249836799266208327
67	7391016289967130	164207682036842086114448097194	164207682036849477130738064324
68	11391634034768010	416635607643573249809932188495	416635607643584641443966956505
69	23941657967808209	1648923729893963761757391941910	1648923729893987703415359750119
70	36917161577580590	4202708638020645946818199797966	4202708638020682863979777378556
71	77586381466034947	16592589875613158504531727357741	16592589875613236090913193392688
72	120189309691294216	42473372537692204736714260167959	42473372537692324926023951462175
73	251528935349306793	167295424464203990256343738221951	167295424464204241785279087528744
74	389800782399677001	430006772381311021662645700992080	430006772381311411463428100669081
75	815741140338068227	1689911835064563934489030380281628	1689911835064564750230170718349855
76	1269537925991351156	4360786726830838778703764330000384	4360786726830840048241690321351540
77	2646489896299591485	17100609751074141570684664508176881	17100609751074144217174560807768366
78	4120240983149128308	44294354185222182700528141004393441	44294354185222186820769124153521749
79	8588824555686539622	173335468778163758926743919095416928	173335468778163767515568474781956550
80	13423903573385498107	450600427378156832136079227317086424	450600427378156845559982800702584531
81	27882748457230290862	1759767313496477928067387728205946251	1759767313496477955950136185436237113
82	43593968512517811907	4590528948690471561022560959260371308	4590528948690471604616529471778183215
83	90545956172141260398	17892924987803326734253890021984886912	17892924987803326824799846194126147310
84	142077351102286455091	46830869858741159117889452362170508243	46830869858741159259966803464456963334
85	294122275423916054352	182194157793655704500115198467223336560	182194157793655704794237473891139390912
86	461655253463248942128	478379522345454678848216263339209430135	478379522345454679309871516802458372263
87	955666449267540395221	1857742280338673466601776204453659906368	1857742280338673467557442653721200301589
88	1505041735231994609714	4892807796459916527756662912397080793588	4892807796459916529261704647629075403302
89	3105981799108470323147	18967377099179003865864655797569778746527	18967377099179003868970637596678249069674
90	4892884042870228987320	50103146420285113734925982237614318781047	50103146420285113739818866280484547768367
91	10097190706324159336800	193898555422930446991054484557154282219435	193898555422930447001151675263478441556235
92	15955816379863267567356	513654043751710294717723475674321178695904	513654043751710294733679292054184446263260
93	32832697580700874763572	1984557489015003230921269397197621565592352	1984557489015003230954102094778322440355924
94	51896703593122831089656	5271743914770706257960929202832187654294339	5271743914770706258012825906425310485383995
95	106785552739916704811839	20335387509472990198568080384836453337202925	20335387509472990198674865937576370042014764
96	169281344462058446325058	54162175051500719402254938276901062628676995	54162175051500719402424219621363121075002053
97	347387515383940750498193	208602785663318655582652789289307612217740815	20860278566331865583000176804691552968239008
98	550829851333133859420094	557028727906484285338942895344159419431573208	557028727906484285339493725195492553290993302
99	1130336590391716286395368	2142136450298921147960563205940582654277126951	2142136450298921147961693542530974370563522319
100	1797192677522993383492050	5734313151200075267208843400877477986664415189	5734313151200075267210640593555000980047907239

Equations 79–81 can be evaluated under the criterion for centroidal 3D-trees (eq. 68). Suppose that we have obtained the generating functions, i.e., $a(x) = \sum_{k=0}^{m} \alpha_k x^k$, $c(x^2) = \sum_{k=0}^{m} \gamma_k x^{2k}$, and $b(x) = \sum_{k=0}^{m} \beta_k x^k$, where m is tentatively fixed. After the introduction of these generating functions into eqs. 79–81, we obtain $\widehat{B}(x)^{(m)}$, $\widehat{A}(x)^{(m)}$, and $\widehat{C}(x)^{(m)}$, respectively. We expand the equation $\widehat{B}(x)^{(m)}$ etc. and adopt the coefficients of x^{2m+1} and x^{2m+2} appearing in each of the expanded equations. Let the symbol coeff($\widehat{B}(x)^{(m)}, x^{2m+1}$) etc. represent the coefficient of the term x^{2m+1}. Then, we obtain the following coefficients:

$$\widehat{B}_{2m+1} = \text{coeff}(\widehat{B}(x)^{(m)}, x^{2m+1}) \quad (82)$$
$$\widehat{A}_{2m+1} = \text{coeff}(\widehat{A}(x)^{(m)}, x^{2m+1}) \quad (83)$$
$$\widehat{C}_{2m+1} = \text{coeff}(\widehat{C}(x)^{(m)}, x^{2m+1}) \quad (84)$$

for odd carbon contents as well as the following coefficients:

$$\widehat{B}_{2m+2} = \text{coeff}(\widehat{B}(x)^{(m)}, x^{2m+2}) \quad (85)$$
$$\widehat{A}_{2m+2} = \text{coeff}(\widehat{A}(x)^{(m)}, x^{2m+2}) \quad (86)$$
$$\widehat{C}_{2m+2} = \text{coeff}(\widehat{C}(x)^{(m)}, x^{2m+2}) \quad (87)$$

for even carbon contents. The program for evaluating these coefficients was written on the same line as the programs "CentrSIA1-100.mpl" and "CentrSIC1-100.mpl". The execution results were identical with the data listed in Table 3.

6 Alkanes as Bicentroidal 3D-Trees

6.1 Two-Nodal Promolecules into Bicentroidal Alkanes

Two-nodal promolecules described in Subsection 2.2 are converted into bicentroidal alkanes, where the two proligands of each two-nodal promolecule are replaced by alkyl ligands described in Section 3.

In a two-nodal promolecule **41** derived from the **K**-skeleton **39**, for example, the proligands X and Y are replaced by a n-propyl ($CH_2CH_2CH_3$) and an isopropyl ligand ($CH(CH_3)_2$) respectively, as shown in Fig. 7. Thereby, the promolecule is converted into 2-methylpentane (**50**) as a bicentroidal alkane of carbon content 6.

Because the promolecule **41** belongs to the $\mathbf{K}_3$-factor group (cf. Fig. 4), the 2-methylpentane is regarded as belonging to the **K**-factor group as an average conformation.

Alkyl ligands, which are enumerated by the generating functions regarded as ligand inventories (eqs. 41–43), are introduced into the promolecule (**41**) under the criterion of bicentroidal 3D-trees (Section 4). When such alkyl ligands have been counted up to carbon content $m = 3$, alkanes of carbon content 6 ($v = 2m = 6$) can be counted. Hence, only one mode of factorization take place: $x^3 \cdot x^3$ for hexane (two n-propyl ligands, **40**; **K**), 2,2-dimethylbutane (two isopropyl ligands, **40**, **K**), and the 2-methylpentane (**50**, $\mathbf{K}_3$).

The procedure described in the preceding paragraph is extended to cover general cases, as described in the following subsections.

39	**41**	**50**
K-skeleton	promolecule	bicentroidal alkane
(**K**(/**K**$_3$))	(two-nodal)	bicentroidal 3D-tree

Figure 7: **K**- or $\mathbf{D}_{\infty h}/\mathbf{C}_{\infty}$-skeleton (**39**) with two substitution positions, a two-nodal promolecule (**41**), and a bicentroidal alkane (**50**).

6.2 Functional Equations for Counting Bicentroidal 3D-Trees

Let **G** be a subgroup of the the factor group **K** (= $\mathbf{D}_{\infty h}/\mathbf{C}_{\infty}$). Let $N_k^{(\mathbf{G})}$ be the number of bicentroidal alkanes (or 3D-trees) which belong to **G** and have carbon content k. On the same line as centroidal 3D-trees, each pair of enantiomeric 3D-trees is counted just once throughout the enumerations described in this paper. In agreement with the definition of bicentroidal 3D-trees, the terms up to x^v are collected to give the following generating functions:

$$N(x)^{(\mathbf{G})} = \sum_{k=0}^{v} N_k^{(\mathbf{G})} x^k, \tag{88}$$

where v runs stepwise from 0 to infinite. The value of $N_k^{(\mathbf{G})}$ is equal to zero when k is odd.

Because each of eqs. 31–35 for two-nodal promolecules corresponds to eq. 88 for bicentroidal 3D-trees, the SIs a_d, c_d, and b_d are replaced by the terms $a(x^d)-1$, $c(x^d)-1$, and $b(x^d)-1$ respectively. Thereby we obtain the following functional equations:

$$\begin{aligned} N(x)^{(\mathbf{K}_1)} &= \frac{1}{4}(b(x)-1)^2 - \frac{1}{4}(b(x^2)-1) \\ &\quad - \frac{1}{4}(a(x)-1)^2 - \frac{1}{4}(c(x^2)-1) + \frac{1}{2}(a(x^2)-1) \qquad (89) \\ N(x)^{(\mathbf{K}_2)} &= \frac{1}{2}(b(x^2)-1) - \frac{1}{2}(a(x^2)-1) \qquad (90) \\ N(x)^{(\mathbf{K}_3)} &= \frac{1}{2}(a(x)-1)^2 - \frac{1}{2}(a(x^2)-1) \qquad (91) \\ N(x)^{(\mathbf{K}_4)} &= \frac{1}{2}(c(x^2)-1) - \frac{1}{2}(a(x^2)-1) \qquad (92) \\ N(x)^{(\mathbf{K})} &= a(x^2)-1. \qquad (93) \end{aligned}$$

The target of this section is to evaluate $N(x)^{(\mathbf{G})}$ (eqs. 89–93) by using eqs. 52–54 under the criterion for bicentroidal 3D-trees. The criterion for bicentroidal 3D-trees requires the relationship:

$$m = \frac{1}{2}v \tag{94}$$

or

$$2m = v. \tag{95}$$

If the value k is tentatively fixed during recursive calculations, eqs. 52–54 are regarded as finite series which have terms up to x^m. They are introduced into the right-hand sides of eqs. 89–93 and the resulting equations are expanded to give respective series $N(x)^{(\mathbf{G},m)}$, each of which is used to give the coefficients of eq. 88. Because of eq. 95, the coefficient of the term x^{2m} in each of the series is effective to determine $N_{2m}^{(\mathbf{G})}$. Let the symbol coeff$(N(x)^{(\mathbf{G},m)}, x^{2m})$ represent the coefficient of the term x^{2m} appearing in the equation $N(x)^{(\mathbf{G},m)}$ after expansion. Then, we obtain the following coefficients:

$$N_{2m}^{(\mathbf{G})} = \text{coeff}(N(x)^{(\mathbf{G},m)}, x^{2m}). \tag{96}$$

Because we take account of the coefficient $N_{2m}^{(\mathbf{G})}$ (eq. 96) only, we can use following functional equations:

$$N(x)^{(\mathbf{K}_1)\prime} = \frac{1}{4}b(x)^2 - \frac{1}{4}b(x^2) - \frac{1}{4}a(x)^2 - \frac{1}{4}c(x^2) + \frac{1}{2}a(x^2) \tag{97}$$

$$N(x)^{(\mathbf{K}_2)\prime} = \frac{1}{2}b(x^2) - \frac{1}{2}a(x^2), \tag{98}$$

$$N(x)^{(\mathbf{K}_3)\prime} = \frac{1}{2}a(x)^2 - \frac{1}{2}a(x^2) \tag{99}$$

$$N(x)^{(\mathbf{K}_4)\prime} = \frac{1}{2}c(x^2) - \frac{1}{2}a(x^2) \tag{100}$$

$$N(x)^{(\mathbf{K})\prime} = a(x^2) \tag{101}$$

in place of eqs. 89–93. Note that eqs. 97–101 are derived from eqs. 31–35 by substituting $a(x^d)$, $c(x^d)$, and $b(x^d)$ for the SIs a_d, c_d, and b_d.

6.3 Recursive Calculation for Counting Bicentroidal 3D-Trees

The program describe in "CentrSIA1-100.mpl" and "CentrSIC1-100.mpl" for evaluating $a(x)$, $c(x^2)$, and $b(x)$ (eqs. 52–54) was also used to evaluate the coefficients $N_k^{(\mathbf{G})}$ (eq. 88). The code for the functional equations shown in eqs. 89–93 was written in a similar way described above. The total program was stored in a file named "BicentrSI1-100B.mpl", which was executed on a display window of the Maple system. The results are shown in Table 4, where the values of $N_k^{(\mathbf{G})}$ for bicentroidal alkanes as 3D-trees are collected up to carbon content $k = 100$.

Maple program for counting bicentroidal 3D-trees, "BicentrSI1-100B.mpl":

```
"Functional Equations for Alkyl Ligands";
ax := 1 + x*a1*c2;
cx := 1+ (1/3)*x^2*c2^3 + (2/3)*x^2*c6;
bx := 1 + (1/3)*x*b1^3 + (2/3)*x*b3;

"Alkanes as Bicentroidal 3D-Trees";
NxK1 := (1/4)*(b1-1)^2 - (1/4)*(b2-1) - (1/4)*(a1-1)^2
- (1/4)*(c2-1) + (1/2)*(a2-1):
NxK2 := (1/2)*(b2-1) - (1/2)*(a2-1):
NxK3 := (1/2)*(a1-1)^2 - (1/2)*(a2-1):
NxK4 := (1/2)*(c2-1) - (1/2)*(a2-1):
NxK  := a2-1:
Bxt := (1/4)*((b1-1)^2 + (b2-1) + (a1-1)^2 + (c2-1)):
```

```
"Initial Values";
a1 := 1; a2 := 1;
b1 := 1; b2 := 1; b3 := 1;
c2 := 1; c4 := 1; c6 := 1;
NK1 := 0; NK2 := 0; NK3 := 0;
NK4 := 0; NK := 0;
Bt := 0;

"Recursive Calculation";
for m from 1 to 50 by 1 do
m:
Cbx:= coeff(bx,x^m):
Cax:= coeff(ax,x^m):
Ccx:= coeff(cx,x^(m*2)):
a1 := a1 + Cax*x^m:
a2 := a2 + Cax*x^(m*2):
b1 := b1 + Cbx*x^m:
b2 := b2 + Cbx*x^(m*2):
b3 := b3 +Cbx*x^(m*3):
c2 := c2 + Ccx*x^(m*2):
c4 := c4 + Ccx*x^(m*4):
c6 := c6 + Ccx*x^(m*6):
n := 2*m:
NK1 := NK1 + coeff(NxK1,x^n)*x^n:
NK2 := NK2 + coeff(NxK2,x^n)*x^n:
NK3 := NK3 + coeff(NxK3,x^n)*x^n:
NK4 := NK4 + coeff(NxK4,x^n)*x^n:
NK := NK + coeff(NxK,x^n)*x^n:
Bt := Bt + coeff(Bxt,x^n)*x^n:
end do:

"Test Digit";
Bt;
Test := NK1 + NK2 + NK3 + NK4 + NK - Bt;

"Print-Out";
for m from 2 to 100 by 2 do
printf("%d & %d & %d & %d & %d & %d  \\\\ \n",
m, coeff(NK1,x^m), coeff(NK2,x^m), coeff(NK3,x^m),
coeff(NK4,x^m), coeff(NK,x^m));
end do;
```

In this program, the first paragraph “Functional Equations for Alkyl Ligands” is concerned with planted 3D-trees. The second paragraph “Alkanes as Bicentroidal 3D-Trees” declares the functional equations $N(x)^{(\mathbf{K}_1)}$ (`NxK1`), $N(x)^{(\mathbf{K}_2)}$ (`NxK2`), $N(x)^{(\mathbf{K}_3)}$ (`NxK3`), $N(x)^{(\mathbf{K}_4)}$ (`NxK4`), and $N(x)^{(\mathbf{K})}$ (`NxK`). The symbol `Bxt` is to calculate the total number of bicentroidal 3D-trees. The third paragraph “Initial Values” gives the initial values for every functional equations. The fourth paragraph “Recursive Calculation” is composed of a `do` loop for recursive calculations. The resulting values at each step of m, which is referred to by the symbol $N(x)^{(\mathbf{G},m)}$ in the text (cf. eqs. 96), are stored as the series denoted by the symbols `NK1`, `NK2`, and so on. Note that `Bt` is a series for storing the results due to the functional equation shown by `Bxt`. Note that m moves from 1 to 50 to calculate the values `NCs`, `NS4`, etc. up to carbon content 100. The fifth paragraph ”Test

Table 4: Numbers of Chiral and Achiral Bicentroidal Alkanes as Stereoisomers

k	$N_k^{(\mathbf{K}_1)}$	$N_k^{(\mathbf{K}_2)}$	$N_k^{(\mathbf{K}_3)}$	$N_k^{(\mathbf{K}_4)}$	$N_k^{(\mathbf{K})}$
2	0	0	0	0	1
4	0	0	0	0	1
6	0	0	1	0	2
8	3	1	3	1	3
10	21	3	10	3	5
12	170	10	28	10	8
14	1290	30	91	30	14
16	9680	88	253	88	23
18	75225	255	820	255	41
20	601020	742	2346	742	69
22	4913646	2157	7381	2157	122
24	41147928	6312	21528	6312	208
26	351434716	18563	68265	18563	370
28	3052406444	54932	201930	54932	636
30	26910605148	163479	642411	163479	1134
32	240339197664	489264	1925703	489264	1963
34	2171034151632	1471692	6140760	1471692	3505
36	19810902096624	4447896	18595851	4447896	6099
38	182415855489644	13500689	59486778	13500689	10908
40	1693333684316928	41140608	181613211	41140608	19059
42	15834517653168865	125818217	582377256	125818217	34129
44	149058121084835254	386050543	1790143530	386050543	59836
46	1411693337070824624	1188093392	5751871140	1188093392	107256
48	13444258974971682096	3666547089	17780359600	3666547089	188576
50	128691508649139937350	11344058829	57230718681	11344058829	338322
52	1237676126323847582232	3518032336	17757925626	3518032336	596252
54	11955155209909770194588	1093390971119	5730209873 11	10933909711 9	1070534
56	115946610491159850069600	340508394528	1787084924878	340508394528	1890548
58	1128738527373066868688910	1062419370490	5768342184165	1062419370490	3396570
60	11026844701941179705888430	3320666310903	18053484671778	3320666310903	6008908
62	108076850325850215726768250	10395996250010	58339609048020	10395996250010	10801816
64	1062546355974610837369643571	32596713516873	183153617487435	32596713516873	19139155
66	104764798153309942380461219 40	1023546593566690	5924555509546916	1023546593566690	34422537
68	10357642512538423142140799055 5	321832884381903	1865052313774653	321832884381903	61074583
70	102663642287285292846009916184 4	1013230630964436	6038377871932071	1013230630964436	109894294
72	10200477451834273436225561185100	3193818534035050	19054887836824378	3193818534035050	195217253
74	1015816722992133916821756067171 20	1007877177202180	6174245747013891 0	1007877177202180	351404205
76	101379168252567599696381861071043 84	31840095204449021	1952583059473756 86	31840095204449021	624913284
78	10138463629083017138288148518338330	1006899375100483 85	6331409002825700 01	1006899375100483 85	1125291874
80	101587632316921571608122788467850571	3187281469818446 79	2006184915267847485	3187281469818446 79	2003090071
82	101979600192005851301371897648296 8640	1009849492883144730	6509464275862265941	1009849492883144730	3608175239
84	102553630284724014535747069454998315 29	3202399570304430261	2066235695850326325 6	3202399570304430261	6428430129
86	103304260659299978074713484823995926 18	1016387035246917805 9	6708289172207088084 6	1016387035246917805 9	11582995444
88	1042273130631919367912051902439879332026	3228425514031800267 9	2132752949088437887 20	3228425514031800267 9	20653101216
90	1053197574905581889101959695381302817560 0	1026254147140742501 95	6927996087154154555 55	1026254147140742501 95	37223637886
92	1065796003713350563728592832217234793 26706	3264653126285412532 82	2205819023251906595 676	3264653126285412532 82	66420162952
94	1080057924052835851968590047147334594849394	1039258352830707100287	7168899247099742388600	1039258352830707100287	119740546576
96	1095981528487151787034394158240084016584014	3310561173602401804486	2285573104119297979716	3310561173602401804486	213802390264
98	1113573076689154578892749482633494818885534 78	1055259719997153894444 46	7431490763407299302212 8	1055259719997153894444 46	385525375648
100	1132846394716372419231278583317989278246204150	3365778356774535211759 95	2372205488904920292243 00	3365778356774535211759 5	688796847976

Digit" confirms the validity of the results, where the result stored in the series `Bt` is used as a standard. Hence `Test` should be equal to zero if the present calculations are correct. The last paragraph "Print-Out" declares a `do` loop for printing out the values in a tabular form up to carbon content 100 (only for the cases of even carbon contents).

7 Alkanes as Balanced and Unbalanced 3D-Trees

We have recently developed the dichotomy between balanced and unbalanced trees (or 3D-trees) as a new dichotomy which is applicable to the enumeration of trees or 3D-trees. The new dichotomy provides us a tool for categorizing bicentroidal 3D-trees further into bicentroidal & balanced 3D-trees (or simply balanced 3D-trees) and bicentroidal & unbalanced 3D-trees. The present section is devoted to discuss this categorization in comparison with the present symmetry-itemization.

7.1 Bicentroidal & Balanced 3D-Trees

The new dichotomy is based on the absence or presence of a balance-edge, in which the two branch incident to the balance-edge are congruent to each other under the action of the factor group $\mathbf{K} (= \mathbf{D}_{\infty h}/\mathbf{C}_{\infty})$. A 3D-tree which has a balance-edge is called a *balanced 3D-tree*; otherwise a 3D-tree is called an *unbalanced 3D-tree*.

Because balanced 3D-trees are always bicentroidal 3D-trees, the inspection of Fig. 4 teaches us that there are three cases, i.e., $\mathbf{K}_2$ ($= \mathbf{D}_\infty/\mathbf{C}_\infty$) for p—p (paired with $\overline{\text{p}}$—$\overline{\text{p}}$), $\mathbf{K}_4$ ($= \mathbf{C}_{\infty h}/\mathbf{C}_\infty$) for p—$\overline{\text{p}}$, and $\mathbf{K}$ ($= \mathbf{D}_{\infty h}/\mathbf{C}_\infty$) for X—X. The summation of eqs. 32, 34, and 35 gives the following CI-CF$_B^{(AC)}$:

$$\begin{aligned} \text{CI-CF}_B^{(AC)}(\mathbf{K}, \$_d) &= \text{PCI-CF}(\mathbf{K}_2, \$_d) + \text{PCI-CF}(\mathbf{K}_4, \$_d) + \text{PCI-CF}(\mathbf{K}, \$_d) \\ &= \frac{1}{2}(b_2 + c_2). \end{aligned} \tag{102}$$

Among the balanced 3D-trees, achiral ones are $\mathbf{K}_4$ ($= \mathbf{C}_{\infty h}/\mathbf{C}_\infty$) for p—$\overline{\text{p}}$ and $\mathbf{K}$ ($= \mathbf{D}_{\infty h}/\mathbf{C}_\infty$) for X—X. They are summed up to give the following CI-CF$_B^{(A)}$;

$$\begin{aligned} \text{CI-CF}_B^{(A)}(\mathbf{K}, \$_d) &= \text{PCI-CF}(\mathbf{K}_4, \$_d) + \text{PCI-CF}(\mathbf{K}, \$_d) \\ &= \frac{1}{2}(a_2 + c_2). \end{aligned} \tag{103}$$

Chiral balanced 3D-trees are left behind as follows:

$$\begin{aligned} \text{CI-CF}_B^{(C)}(\mathbf{K}, \$_d) &= \text{PCI-CF}(\mathbf{K}_2, \$_d) \\ &= \frac{1}{2}(b_2 - a_2). \end{aligned} \tag{104}$$

Let $B_k^{(\text{AC})}$ be the number of achiral balanced 3D-trees plus enantiomeric pairs of chiral balanced 3D-trees of carbon content k; let $B_k^{(\text{A})}$ be the number of achiral balanced 3D-trees of carbon content k; and let $B_k^{(\text{C})}$ be the number of achiral and chiral balanced 3D-trees of carbon content k, where each pair of enantiomers is counted just once. Then, they appear as the coefficients of the following series:

$$B(x)^{(\text{AC})} = \sum_{k=1}^{\infty} B_k^{(\text{AC})} x^k \tag{105}$$

$$B(x)^{(\text{A})} = \sum_{k=1}^{\infty} B_k^{(\text{A})} x^k \tag{106}$$

$$B(x)^{(\text{C})} = \sum_{k=1}^{\infty} B_k^{(\text{C})} x^k, \tag{107}$$

where the coefficient of x^k is equal to 0 if k is odd.

To evaluate the counting series represented by eqs. 105–107, we derive functional equations by substituting $a(x^d) - 1$, $c(x^d) - 1$, and $b(x^d) - 1$ for the SIs (a_d, c_d, and b_d) appearing in the CI-CFs (eqs. 102–104). Thereby, we obtain the following functional equations:

$$B(x)^{(\text{AC})} = \frac{1}{2}\{(b(x^2) - 1) + (c(x^2) - 1)\} \tag{108}$$

$$B(x)^{(\text{A})} = \frac{1}{2}\{(a(x^2) - 1) + (c(x^2) - 1)\} \tag{109}$$

$$B(x)^{(\text{C})} = \frac{1}{2}\{(b(x^2) - 1) - (a(x^2) - 1)\}. \tag{110}$$

Because we have already obtained the coefficients of every terms of eqs. 41–43, they are introduced into eqs. 108–110. The resulting equations are expanded to give $B_k^{(\text{AC})}$, $B_k^{(\text{A})}$, and $B_k^{(\text{C})}$.

The code for evaluating $a(x)$, $c(x^2)$, and $b(x)$ (eqs. 52–54) was also used to evaluate the coefficients $B_k^{(AC)}$ (eq. 105), $B_k^{(A)}$ (eq. 106), and $B_k^{(C)}$ (eq. 107). The total program was stored in a file named "BiBalSI1-100.mpl", which was executed on a display window of the Maple system. The results are shown in Table 5, where the values are collected up to carbon content $k = 100$.

Maple program for counting bicentroidal & balanced 3D-trees, "BiBalSI1-100.mpl":

```
"Functional Equations for Alkyl Ligands";
ax := 1 + x*a1*c2;
cx := 1+ (1/3)*x^2*c2^3 + (2/3)*x^2*c6;
bx := 1 + (1/3)*x*b1^3 + (2/3)*x*b3;

"Alkanes as Bicentroidal and Ballanced 3D-Trees";
BxAC := (1/2)*(b2-1) + (1/2)*(c2-1):
BxA := (1/2)*(a2-1) + (1/2)*(c2-1):
BxC := (1/2)*(b2-1) - (1/2)*(a2-1):

"Initial Values";
a1 := 1; a2 := 1;
b1 := 1; b2 := 1; b3 := 1;
c2 := 1; c4 := 1; c6 := 1;
BAC := 0; BA := 0; BC := 0;

"Recursive Calculation";
for m from 1 to 50 by 1 do
m:
Cbx:= coeff(bx,x^m):
Cax:= coeff(ax,x^m):
Ccx:= coeff(cx,x^(m*2)):
a1 := a1 + Cax*x^m:
a2 := a2 + Cax*x^(m*2):
b1 := b1 + Cbx*x^m:
b2 := b2 + Cbx*x^(m*2):
b3 := b3 +Cbx*x^(m*3):
c2 := c2 + Ccx*x^(m*2):
c4 := c4 + Ccx*x^(m*4):
c6 := c6 + Ccx*x^(m*6):
n := 2*m:
BAC := BAC + coeff(BxAC,x^n)*x^n:
BA := BA + coeff(BxA,x^n)*x^n:
BC := BC + coeff(BxC,x^n)*x^n:
end do:

"Print-Out";
for m from 2 to 100 by 2 do
printf("%d & %d & %d & %d \\\\ \n",
m, coeff(BA,x^m), coeff(BC,x^m), coeff(BAC,x^m));
end do;
```

In this program, we use the criterion for bicentroidal 3D-trees (i.e., eq. 95) in the evaluation of eqs. 108–110. However, the same results can be obtained without the use of the criterion. Thus, the lines concerned with `BAC`, `BA`, `BC` are deleted from the paragraphs "Initial Values" and "Recursive Calculation" of the above program "BiBalSI1-100.mpl"; and the paragraph "Print-Out" is rewritten as follows:

Table 5: Numbers of Bicentroidal & Balanced Alkanes as Stereoisomers

k	$B_k^{(A)}$	$B_k^{(C)}$	$B_k^{(AC)}$
2	1	0	1
4	1	0	1
6	2	0	2
8	4	1	5
10	8	3	11
12	18	10	28
14	44	30	74
16	111	88	199
18	296	255	551
20	811	742	1553
22	2279	2157	4436
24	6520	6312	12832
26	18933	18563	37496
28	55568	54932	110500
30	164613	163479	328092
32	491227	489264	980491
34	1475197	1471692	2946889
36	4453995	4447896	8901891
38	13511597	13500689	27012286
40	41159667	41140608	82300275
42	125852346	125818217	251670563
44	386110379	386050543	772160922
46	1188200648	1188093392	2376294040
48	3666735665	3666547089	7333282754
50	11344397151	11344058829	22688455980
52	35180919588	35180323336	70361242924
54	109340167653	109339097119	218679264772
56	340510285076	340508394528	681018679604
58	1062422767060	1062419370490	2124842137550
60	3320672319811	3320666310903	6641338630714
62	10396007051826	10395996250010	20792003301836
64	32596732656028	32596713516873	65193446172901
66	102354693779227	102354659356690	204709353135917
68	321832945456486	321832884381903	643665829838389
70	1013230740858730	1013230630964436	2026461371823166
72	3193818729252303	3193818534035050	6387637263287353
74	10078773528606385	10078773177202180	20157546705808565
76	31840095829362305	31840095204449021	63680191033811326
78	100689938635340259	100689937510048385	201379876145388644
80	318728148984934750	318728146981844679	637456295966779429
82	1009849496491319969	1009849492883144730	2019698989374464699
84	3202399576732860390	3202399570304430261	6404799147037290651
86	10163870364052173503	10163870352469178059	20327740716521351562
88	32284255160971103895	32284255140318002679	64568510301289106574
90	102625414751297888081	102625414714074250195	205250829465372138276
92	326465312694961416234	326465312628541253282	652930625323502669516
94	1039258352950447646863	1039258352830707100287	2078516705781154747150
96	3310561173816204194750	3310561173602401804486	6621122347418605999236
98	10552597200357064320094	10552597199971538944446	21105194400328603264540
100	33657783568434148965571	33657783567745352117595	67315567136179501083166

```
"Print-Out";
for m from 2 to 100 by 2 do
printf("%d & %d & %d & %d \\\\ \n",
m, coeff(BxA,x^m), coeff(BxC,x^m), coeff(BxAC,x^m));
end do;
```

This is because eqs. 108–110 implicitly satisfy the criterion in the form of the functions $a(x^2)$, $c(x^2)$, and $b(x^2)$ due to the SIs a_2, c_2, and b_2.

7.2 Bicentroidal & Unbalanced 3D-Trees

By the inspection of Fig. 4, we find that bicentroidal & unbalanced 3D-trees belong to $\mathbf{K}_1$ (X—p or p—q) or $\mathbf{K}_3$ (X—Y), where the two ligands of each pair X/p, p/q, and X/Y have the same carbon content. The summation of eq. 31 and eq. 33 gives the following

CI-CF$_U^{(AC)}$:

$$\begin{aligned} \text{CI-CF}_U^{(AC)}(\mathbf{K}, \$_d) &= \text{PCI-CF}(\mathbf{K}_1, \$_d) + \text{PCI-CF}(\mathbf{K}_3, \$_d) \\ &= \frac{1}{4}b_1^2 - \frac{1}{4}b_2 + \frac{1}{4}a_1^2 - \frac{1}{4}c_2. \end{aligned} \tag{111}$$

Because achiral bicentroidal & unbalanced 3D-trees belong to $\mathbf{K}_3$ (X—Y), eq. 33 gives the following CI-CF$_U^{(A)}$:

$$\begin{aligned} \text{CI-CF}_U^{(A)}(\mathbf{K}, \$_d) &= \text{PCI-CF}(\mathbf{K}_3, \$_d) \\ &= \frac{1}{2}a_1^2 - \frac{1}{2}a_2, \end{aligned} \tag{112}$$

Because chiral bicentroidal & unbalanced 3D-trees belong to $\mathbf{K}_1$ (X—p or p—q), eq. 31 gives the following CI-CF$_U^{(C)}$:

$$\begin{aligned} \text{CI-CF}_U^{(C)}(\mathbf{K}, \$_d) &= \text{PCI-CF}(\mathbf{K}_1, \$_d) \\ &= \frac{1}{4}b_1^2 - \frac{1}{4}b_2 - \frac{1}{4}a_1^2 - \frac{1}{4}c_2 + \frac{1}{2}a_2. \end{aligned} \tag{113}$$

Let $\widetilde{U}_k^{(\mathrm{AC})}$, $\widetilde{U}_k^{(\mathrm{A})}$, and $\widetilde{U}_k^{(\mathrm{C})}$ be the number of achiral and chiral bicentroidal & unbalanced 3D-trees the number of achiral bicentroidal & unbalanced 3D-trees, the number of chiral bicentroidal & unbalanced 3D-trees, where each number is concerned with carbon content k and a pair of enantiomers is counted just once. Then, they appear as the coefficients of the following series:

$$\widetilde{U}_k^{(\mathrm{AC})} = \sum_{k=1}^{\infty} \widetilde{U}_k^{(\mathrm{AC})} x^k \tag{114}$$

$$\widetilde{U}_k^{(\mathrm{A})} = \sum_{k=1}^{\infty} \widetilde{U}_k^{(\mathrm{A})} x^k \tag{115}$$

$$\widetilde{U}_k^{(\mathrm{C})} = \sum_{k=1}^{\infty} \widetilde{U}_k^{(\mathrm{C})} x^k \tag{116}$$

where the coefficient of x^k is equal to 0 if k is odd.

To evaluate the counting series represented by eqs. 114–116, we derive functional equations by substituting $a(x^d) - 1$, $c(x^d) - 1$, and $b(x^d) - 1$ for the SIs (a_d, c_d, and b_d) appearing in the CI-CFs (eqs. 111–113). Thereby, we obtain the following functional equations:

$$\widetilde{U}(x)^{(\mathrm{AC})} = \frac{1}{4}(b(x)-1)^2 - \frac{1}{4}(b(x^2)-1) + \frac{1}{4}(a(x)-1)^2 - \frac{1}{4}(c(x^2)-1) \tag{117}$$

$$\widetilde{U}(x)^{(\mathrm{A})} = \frac{1}{2}(a(x)-1)^2 - \frac{1}{2}(a(x^2)-1), \tag{118}$$

$$\begin{aligned} \widetilde{U}(x)^{(\mathrm{C})} &= \frac{1}{4}(b(x)-1)^2 - \frac{1}{4}(b(x^2)-1) \\ &\quad - \frac{1}{4}(a(x)-1)^2 - \frac{1}{4}(c(x^2)-1) + \frac{1}{2}(a(x^2)-1), \end{aligned} \tag{119}$$

After eqs. 52–54 are introduced into $\widetilde{U}(x)^{(\mathrm{AC})}$ (eq. 117), $\widetilde{U}(x)^{(\mathrm{A})}$ (eq. 118), and $\widetilde{U}(x)^{(\mathrm{C})}$ (eq. 119), they are evaluated under the criterion for bicentroidal 3D-trees (i.e., eq. 95). If

Table 6: Numbers of Bicentroidal & Unbalanced Alkanes as Stereoisomers

k	$\widetilde{U}_k^{(A)}$	$\widetilde{U}_k^{(C)}$	$\widetilde{U}_k^{(AC)}$
2	0	0	0
4	0	0	0
6	1	0	1
8	3	3	6
10	10	21	31
12	28	170	198
14	91	1290	1381
16	253	9680	9933
18	820	75225	76045
20	2346	601020	603366
22	7381	4913646	4921027
24	21528	41147928	41169456
26	68265	351434716	351502981
28	201930	3052406444	3052608374
30	642411	26910605148	26911247559
32	1925703	240339197664	240341123367
34	6140760	2171034151632	2171040292392
36	18595851	19810902096624	19810920692475
38	59486778	182415855489644	182415914976422
40	181613211	1693333684316928	1693333865930139
42	582377256	15834517653168865	15834518235546121
44	1790143530	149058121084835254	149058122874978784
46	5751871140	1411693370708246 24	1411693342822695764
48	17788359600	134442589749716820 96	134442589927520416696
50	57230718681	1286915086491339373 50	1286915087063706560 31
52	177757925626	12376761263284755822 32	12376761265062335078 58
54	573020987311	11955155209909770194588	11955155210482791181899
56	1787084924878	11594661049159850069600	11594661049294693494478
58	5768342184165	11287385273730666888689 10	11287385273788350308737 5
60	18053484671778	11026844701944179705888430	11026844701959233190560208
62	58339609048020	10807685032585021572678280 96	10807685032590855533816070
64	183153617487435	10625463559746108373696435 71	10625463559749739909871310 06
66	592455509546916	10476479815330994238046121940	10476479815331586693555668856
68	1865052313774653	10357642512538423142140799 0955	10357642512538609647372176 5608
70	6038377871932071	10266364228728529284600991618 44	10266364228728589668379710939 15
72	19054887836824378	10200477451834273436225561185100	10200477451834292491113398009478
74	61742457470138910	10158167229921345342463307685603 0	10158167229921345342463307685603 0
76	195258305947375686	10137916825256759696381861071043 84	10137916825256761648964920544800 70
78	633140900282570001	10138463629083017713828814851833 330	10138463629083017771429044800953331
80	2006184915267847485	10158763231692157160812278467850571	10158763231692157361430770373569056
82	6509464275862265941	10197960019200585130137189764829686 40	10197960019200585195231832523453 4581
84	20662356958503263256	10255363028472401453574706945499831529	10255363028472401474237063904003094785
86	67082891722070880846	10330426065952999780747143484239592618	10330426065952999787455432656447047 3464
88	213275294908843788720	10422731306319193679120519024398793320 26	10422731306319193681253271973487231207 46
90	692799608715415455555	10531975749055818891019596953813028175600	10531975749055818891712396562528443631155
92	2205819023251906595676	10657960037133505637285928322172347932670 6	10657960037133505637506510224497538592238 2
94	7168899247099742388600	10800579240528358519976859004714733459484939 4	10800579240528358519757589463944343372379 94
96	22855731041192979799716	10959815284871517870343941582400840165844014	10959815284871517870366797313442033145643730
98	74314907634072993022128	11135730766891545788927494826334948188855347 8	11135730766891545788934926317098355488157560 6
100	237220548890492029224300	11328463947163724192312785833179892782462041 50	11328463947163724192315158038668797702754284 50

the maximum value of k is tentatively fixed to be m during recursive calculations, eqs. 52–54 are regarded as finite series which have terms up to x^m. They are introduced into the right-hand sides of eqs. 117–119 and the resulting equations are expanded to give respective series $\widetilde{U}(x)^{(\mathrm{AC},\,\mathrm{m})}$, etc., each of which is used to give the coefficients of eq. 114, etc. Because of eq. 95, the coefficient of the term x^{2m} in each of the series is effective to determine $\widetilde{U}_{2m}^{(\mathrm{AC})}$, etc. Let the symbol $\mathrm{coeff}(\widetilde{U}(x)^{(\mathrm{AC},\,\mathrm{m})}, x^{2m})$ represent the coefficient of the term x^{2m} appearing in the equation $\widetilde{U}(x)^{(\mathrm{AC},\,\mathrm{m})}$ after expansion. Then, we obtain the following coefficients:

$$\widetilde{U}_{2m}^{(\mathrm{AC})} = \mathrm{coeff}(\widetilde{U}(x)^{(\mathrm{AC},\,\mathrm{m})}, x^{2m}) \tag{120}$$

$$\widetilde{U}_{2m}^{(\mathrm{A})} = \mathrm{coeff}(\widetilde{U}(x)^{(\mathrm{A},\,\mathrm{m})}, x^{2m}) \tag{121}$$

$$\widetilde{U}_{2m}^{(\mathrm{C})} = \mathrm{coeff}(\widetilde{U}(x)^{(\mathrm{C},\,\mathrm{m})}, x^{2m}) \tag{122}$$

The code for evaluating $a(x)$, $c(x^2)$, and $b(x)$ (eqs. 52–54) was the same as used previously. The program for the functional equations shown in eqs. 117–119 was written in a similar way described above. The total program was stored in a file named "BiUnBSI1-100.mpl", which was executed on a display window of the Maple system. The results are shown in Table 6, where the values are collected up to carbon content $k = 100$.

Maple program for counting bicentroidal & unbalanced 3D-trees, "BiUnBSI1-100.mpl":

```
"Functional Equations for Alkyl Ligands";
ax := 1 + x*a1*c2;
cx := 1+ (1/3)*x^2*c2^3 + (2/3)*x^2*c6;
bx := 1 + (1/3)*x*b1^3 + (2/3)*x*b3;

"Alkanes as Bicentroidal Unbalanced 3D-Trees";
BUxAC := (1/4)*(b1-1)^2 - (1/4)*(b2-1) + (1/4)*(a1-1)^2 - (1/4)*(c2-1):
BUxA := (1/2)*(a1-1)^2 - (1/2)*(a2-1):
BUxC := (1/4)*(b1-1)^2 - (1/4)*(b2-1) - (1/4)*(a1-1)^2
- (1/4)*(c2-1) + (1/2)*(a2-1):

"Initial Values";
a1 := 1; a2 := 1;
b1 := 1; b2 := 1; b3 := 1;
c2 := 1; c4 := 1; c6 := 1;
BUAC := 0; BUA := 0; BUC := 0;

"Recursive Calculation";
for m from 1 to 50 by 1 do
m:
Cbx:= coeff(bx,x^m):
Cax:= coeff(ax,x^m):
Ccx:= coeff(cx,x^(m*2)):
a1 := a1 + Cax*x^m:
a2 := a2 + Cax*x^(m*2):
b1 := b1 + Cbx*x^m:
b2 := b2 + Cbx*x^(m*2):
b3 := b3 +Cbx*x^(m*3):
c2 := c2 + Ccx*x^(m*2):
c4 := c4 + Ccx*x^(m*4):
c6 := c6 + Ccx*x^(m*6):
n := 2*m:
BUAC := BUAC + coeff(BUxAC,x^n)*x^n:
BUA := BUA + coeff(BUxA,x^n)*x^n:
BUC := BUC + coeff(BUxC,x^n)*x^n:
end do:

"Print-Out";
for m from 2 to 100 by 2 do
printf("%d & %d & %d & %d   \\\\ \n",
m, coeff(BUA,x^m), coeff(BUC,x^m), coeff(BUAC,x^m));
end do;
```

8 Discussion

8.1 Examination of Alkanes of Carbon Content 8

To confirm the validity of the present enumeration, let us examine centroidal alkanes of carbon content 8. The ($k = 8$)-row of Table 3 shows that there exist seven achiral centroidal alkanes ($\widehat{A}_8 = 7$), which are categorized into six $\mathbf{C}_s$-stereoisomers ($N_8^{(\mathbf{C}_s)} = 6$) and one $\mathbf{C}_{3v}$-stereoisomers ($N_8^{(\mathbf{C}_{3v})} = 1$), as shown in the ($k = 8$)-row of Table 1. The ($k = 8$)-row of Table 3 shows there exists one chiral centroidal alkane ($\widehat{C}_8 = 1$), which belongs to $\mathbf{C}_1$-symmetry ($N_8^{(\mathbf{C}_1)} = 1$), as shown in the ($k = 8$)-row of Table 2. These centroidal

alkanes are depicted at the upper part of Fig. 8. Note that an arbitrary enantiomer is depicted for a representative of each enantiomeric pair of chiral alkanes throughout the present discussion.

The centroidal alkanes depicted in Fig 8 can be correlated to the promolecules depicted in Fig. 2. The six $\mathbf{C}_s$-stereoisomers (**51**–**56**) are assigned to the $\mathbf{C}_s$-promolecule (**11**). There appear no $\mathbf{C}_s$-stereoisomers of carbon content 8 which correspond to the other $\mathbf{C}_s$-promolecules (**12**–**14**). The criterion for centroidal 3D-trees (eq. 68) means that the carbon content $k = v = 8$ is generated from $m = 3$ (i.e., $2m + 2 = 8$) so that all of the alkyl ligands incident to each centroid (marked with an asterisk) have carbon contents equal to or less than 3. They are selected from hydrogen, methyl, ethyl, *n*-propyl and isopropyl, which are all achiral. Hence, the other $\mathbf{C}_s$-promolecules (**12**–**14**) do not appear in Fig. 8, because they should contain an enantiomeric pair of chiral proligands. The $\mathbf{C}_{3v}$-stereoisomer of carbon content 8 (**57**) corresponds to the $\mathbf{C}_{3v}$-promolecule (**4**), where we place X = CH_2CH_3 (ethyl) and Y = H (hydrogen). The $\mathbf{C}_1$-stereoisomer of carbon content 8 (**58**) corresponds to the $\mathbf{C}_1$-promolecule (**19**), where we place X = CH_3 (methyl), Y = $CH(CH_3)_2$ (isopropyl), X = $CH_2CH_2CH_3$ (*n*-propyl), and H = H (hydrogen). The other $\mathbf{C}_1$-promolecules listed in Fig. 2 do not appear in Fig 8, because they involve at least one chiral proligand, which does not appear under the criterion $m = 3$ ($< \frac{1}{2}v = 4$).

The bicentroidal alkanes are categorized into bicentroidal & balanced alkanes (Table 5) and bicentroidal & unbalanced alkanes (Table 6). The ($k = 8$)-row of Table 5 shows there exist four achiral bicentroidal & balanced alkanes ($B_8^{(\mathrm{A})} = 4$), which are categorized into one $\mathbf{K}_4$-isomer ($N_8^{(\mathbf{K}_4)} = 1$) and three $\mathbf{K}$-isomers ($N_8^{(\mathbf{K})} = 3$), where the itemized data are found in Table 4. The datum $\widetilde{U}_8^{(\mathrm{A})} = 3$ for achiral bicentroidal & unbalanced alkanes shown in Table 6 correspond to the datum $N_8^{(\mathbf{K}_3)} = 3$ shown in Table 4. The ($k = 8$)-row of Table 5 shows there exists one chiral bicentroidal & balanced alkane ($B_8^{\mathrm{C}} = 1$), which belongs to $\mathbf{K}_2$-symmetry ($N_8^{(\mathbf{K}_2)} = 1$), as shown in the ($k = 8$)-row of Table 4. The datum $\widetilde{U}_8^{(\mathrm{C})} = 3$ for chiral bicentroidal & unbalanced alkanes shown in Table 6 correspond to the datum $N_8^{(\mathbf{K}_1)} = 3$ shown in Table 4. These bicentroidal alkanes are depicted at the lower part of Fig. 8 (below the horizontal double line).

Each of the bicentroidal alkanes depicted in Fig. 8 can be divided into two halves at the edge of the bicentroid (marked with a couple of asterisks). The bicentroidal alkanes of $\mathbf{K}_3$-symmetry (**59**–**61**) correspond to the $\mathbf{K}_3$-promolecule (**41**), where we replace the proligands X and Y by achiral alkyl ligands of carbon content 4 (i.e., *n*-butyl, isobutyl, and *t*-butyl). The bicentroidal alkane of $\mathbf{K}_4$-symmetry (**62**) is a *meso*-compound, which corresponds to the $\mathbf{K}_4$-promolecule (**41**). Note that two halves are *sec*-butyl ligands of an enantiomeric pair. The bicentroidal alkanes of $\mathbf{K}$-symmetry (**63**–**65**) correspond to the $\mathbf{K}$-promolecule (**40**), where we replace the two proligands X by achiral alkyl ligands of carbon content 4 (i.e., *n*-butyl, isobutyl, and *t*-butyl). The bicentroidal alkanes of $\mathbf{K}_1$-symmetry (**66**–**68**) correspond to the $\mathbf{K}_1$-promolecule (**44**), where we replace the proligand X by an achiral alkyl ligand of carbon content 4 (i.e., *n*-butyl, isobutyl, or *t*-butyl) as well as the proligand p by a chiral alkyl ligand of carbon content 4 (i.e., *sec*-butyl). The bicentroidal alkane of $\mathbf{K}_2$-symmetry (**69**) correspond to the $\mathbf{K}_2$-promolecule (**43**), where we replace the proligand p by a chiral alkyl ligand of carbon content 4 (i.e., *sec*-butyl).

It should be noted that the $\mathbf{K}_4$-alkane (**62**) of *meso*-type corresponds to the $\mathbf{K}_2$-alkane (**69**) of chiral type in one-to-one fashion. This type of correspondence holds true in general, as found easily by comparing the corresponding promolecules (i.e., **42** vs. **43**).

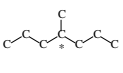 **51** ($\mathbf{C}_s$)	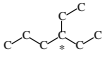 **52** ($\mathbf{C}_s$)	 **53** ($\mathbf{C}_s$)	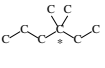 **54** ($\mathbf{C}_s$) achiral $N_8^{(\mathbf{C}_s)} = 6$ (Table 1)
 **55** ($\mathbf{C}_s$)	 **56** ($\mathbf{C}_s$)		
 **57** ($\mathbf{C}_{3v}$)			achiral $N_8^{(\mathbf{C}_{3v})} = 1$ (Table 1)
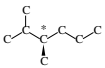 **58** ($\mathbf{C}_1$)			chiral $N_8^{(\mathbf{C}_1)} = 1$ (Table 2)
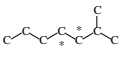 **59** ($\mathbf{K}_3$)	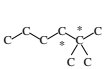 **60** ($\mathbf{K}_3$)	 **61** ($\mathbf{K}_3$)	achiral $N_8^{(\mathbf{K}_3)} = 3$ (Table 4)
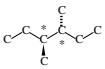 **62** ($\mathbf{K}_4$) (meso)			achiral $N_8^{(\mathbf{K}_4)} = 1$ (Table 4)
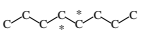 **63** ($\mathbf{K}$)	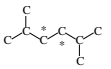 **64** ($\mathbf{K}$)	 **65** ($\mathbf{K}$)	achiral $N_8^{(\mathbf{K})} = 3$ (Table 4)
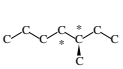 **66** ($\mathbf{K}_1$)	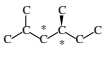 **67** ($\mathbf{K}_1$)	 **68** ($\mathbf{K}_1$)	chiral $N_8^{(\mathbf{K}_1)} = 3$ (Table 4)
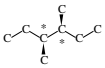 **69** ($\mathbf{K}_2$)			chiral $N_8^{(\mathbf{K}_2)} = 1$ (Table 4)

Figure 8: Symmetry-itemized numbers of alkanes of carbon content 8. A wedged edge is used to show the configuration of the carbon node if necessary. Each carbon with an asterisk is a centroid, while an adjacent pair of carbons with asterisks represents a bicentroid.

Hence, we obtain the following relationship:

$$N_k^{(\mathbf{K}_2)} = N_k^{(\mathbf{K}_4)}. \tag{123}$$

This relationship is confirmed by the inspection of the $N_k^{(\mathbf{K}_2)}$-column and the $N_k^{(\mathbf{K}_4)}$-column of Table 4. Note again that a pair of enantiomeric $N_k^{(\mathbf{K}_2)}$-alkanes (p—p and $\overline{\text{p}}$—$\overline{\text{p}}$) is counted just once in the present enumeration, while an achiral $N_k^{(\mathbf{K}_4)}$-alkane (p—$\overline{\text{p}}$) is spontaneously counted just once.

It is informative to compare the functional equation $N(x)^{(\mathbf{K}_2)}$ (eq. 90) with the functional equation $N(x)^{(\mathbf{K}_4)}$ (eq. 92). Although the two functional equations give the same numbers as shown in eq. 123, they are different in the component terms, i.e., $b(x^2)$ vs. $c(x^2)$, which stem from the sphericities of orbits. The component term $b(x^2)$ is concerned with a two-membered hemispheric orbit, where the chirality fittingness of the orbit permits the accommodation of p—p (paired with $\overline{\text{p}}$—$\overline{\text{p}}$). On the other hand, the component term $c(x^2)$ is concerned with a two-membered enantiospheric orbit, where the chirality fittingness of the orbit permits the accommodation of an enantiomeric pair (p—$\overline{\text{p}}$).

8.2 Examination of Alkanes of Carbon Content 9

All of the alkanes of carbon content 9 are centroidal, because all of the bicentroidal alkanes should have even carbon contents under the criterion shown in eq. 95. The ($k = 9$)-row of Table 3 shows that there exist 21 achiral centroidal alkanes ($\widehat{A}_9 = 21$), which are categorized into 15 $\mathbf{C}_s$-stereoisomers ($N_9^{(\mathbf{C}_s)} = 15$), five $\mathbf{C}_{2v}$-stereoisomers ($N_9^{(\mathbf{C}_{2v})} = 5$), and one $\mathbf{T}_d$-stereoisomers ($N_9^{(\mathbf{T}_d)} = 1$), as shown in the ($k = 9$)-row of Table 1. These centroidal alkanes are depicted in Fig. 9.

The centroidal alkanes depicted in Fig 9 can be correlated to the promolecules depicted in Fig. 2. The $\mathbf{C}_s$-stereoisomers (**70**–**84**) except **73** are assigned to the $\mathbf{C}_s$-promolecule (**11**). The exceptional $\mathbf{C}_s$-stereoisomer (**73**) corresponds to the $\mathbf{C}_s$-promolecules (**12**). There appear no $\mathbf{C}_s$-stereoisomers of carbon content 8 which correspond to the other $\mathbf{C}_s$-promolecules (**13** and **14**), which are referred to as pseudoasymmetry.

The criterion for centroidal 3D-trees (eq. 68) means that the carbon content $k = v = 9$ is generated from $m = 4$ (i.e., $2m + 1 = 9$) so that all of the alkyl ligands incident to each centroid (marked with an asterisk) have carbon contents equal to or less than 4. They are selected from hydrogen, methyl, ethyl, *n*-propyl, isopropyl, *n*-butyl, isobutyl, *sec*-butyl, and *t*-butyl which are achiral except that the *sec*-butyl ligand is chiral. Hence, the $\mathbf{C}_s$-stereoisomers (**70**–**84**) except **73** are composed of such achiral alkyl ligands as having carbon content equal to or less than 4. The exceptional $\mathbf{C}_s$-stereoisomer (**73**) consists of two hydrogens and an enantiomeric pair of *sec*-butyl ligands. Obviously, this case is akin to so-called *meso*-compounds.

The five $\mathbf{C}_{2v}$-stereoisomers of carbon content 9 (**85**–**89**) correspond to the $\mathbf{C}_{2v}$-promolecule (**5**), where the ligands X and Y are selected from the above set of achiral alkyl ligands of carbon content equal to or less than 4. The one $\mathbf{T}_d$-stereoisomer of carbon content 9 (**90**) corresponds to the $\mathbf{T}_d$-promolecule (**2**), where we place X = CH_2CH_3 (ethyl).

The ($k = 9$)-row of Table 3 shows there exist 17 chiral centroidal alkanes ($\widehat{C}_9 = 17$), which are categorized into 16 $\mathbf{C}_1$-stereoisomers ($N_9^{(\mathbf{C}_1)} = 16$) and one $\mathbf{C}_2$-stereoisomer ($N_9^{(\mathbf{C}_2)} = 1$), as shown in the ($k = 9$)-row of Table 2. These centroidal alkanes are depicted

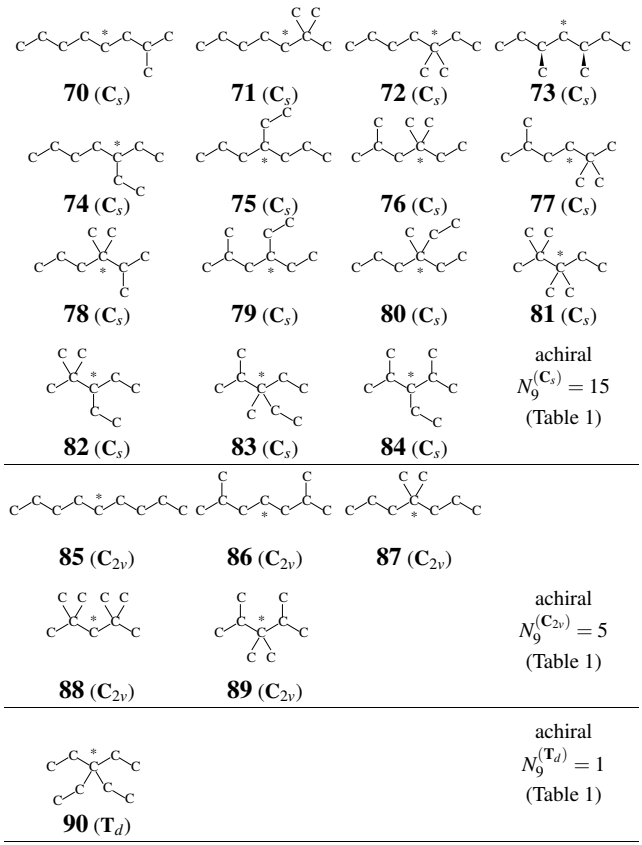

Figure 9: Symmetry-itemized numbers of achiral alkanes of carbon content 9. A wedged edge is used to show the configuration of the carbon node if necessary. Each carbon with an asterisk is a centroid.

in Fig. 10. Note again that an arbitrary enantiomer is depicted for a representative of each enantiomeric pair of chiral alkanes throughout the present discussion.

By the inspection of Fig. 2, the 16 $\mathbf{C}_1$-stereoisomers shown in Fig. 10 are categorized by means of promolecule-types as follows: $\mathbf{C}_1$-stereoisomers of **17**-type (**91**, **97**, **101**, **102**, **103**, and **104**); $\mathbf{C}_1$-stereoisomers of **19**-type (**92**, **93**, **94**, **98**, **102**, **105**, and **106**); and $\mathbf{C}_1$-stereoisomers of **20**/**21**-type (**95**/**96** and **99**/**100**). Note that the promolecules **20** and **21**, which are linked with a brace, are diastereomeric to each other. The one $\mathbf{C}_2$-stereoisomer (**107**) is ascribed to the $\mathbf{C}_2$-promolecule of **15**-type.

On the same line as achiral centroidal alkanes listed in Fig. 9, the substituents of the chiral centroidal alkanes listed in Fig. 10 are selected from hydrogen, methyl, ethyl, *n*-propyl, isopropyl, *n*-butyl, isobutyl, *sec*-butyl, and *t*-butyl, which are achiral except that the *sec*-butyl ligand is chiral. These modes of substitution is in agreement with the criterion for centroidal 3D-trees (eq. 68), which means that all of the alkyl ligands incident to each centroid (marked with an asterisk) have carbon contents equal to or less than 4, where the upper limit $m = 4$ generates the carbon content $2m + 1 = 9$ or $2m + 2 = 10$.

The one $\mathbf{C}_2$-stereoisomer (**107**) shown in Fig. 10 corresponds to the $\mathbf{C}_s$-stereoisomer (**73**), which is akin to so-called *meso*-compounds, as shown in Fig. 9. This type of correspondence holds true in general, as found easily by comparing between the corresponding promolecules, i.e., the $\mathbf{C}_2$-promolecule **15** and the $\mathbf{C}_s$-promolecule **12**.

8.3 Special Cases to be Commented

The $\mathbf{T}_d$-column of Table 1 lists the numbers of achiral centroidal alkanes corresponding to the promolecule **2** shown in Fig. 2. The four achiral proligands (X's) of the same kind in **2** are selected so that the number of $\mathbf{T}_d$-alkanes of carbon content $4n+1$ ($N_{4n+1}^{(\mathbf{T}_d)}$) is equal to the number of achiral alkyl ligands of carbon content n. Note that if the notation must be adjusted in agreement with eq. 68, we should put $m = 2n$ so as to satisfy $4n+1 = 2m+1$. For example, the value $N_1^{(\mathbf{T}_d)} = 1$ corresponds to a set of four hydrogens; $N_5^{(\mathbf{T}_d)} = 1$ to a set of four methyls; $N_9^{(\mathbf{T}_d)} = 1$ to a set of four ethyls (cf. **90**); $N_{13}^{(\mathbf{T}_d)} = 2$ to a set of four *n*-propyls and a set of four isopropyls; $N_{17}^{(\mathbf{T}_d)} = 3$ to a set of four *n*-butyl, a set of four isobutyls, and a set of four *t*-butyls; as well as $N_{17}^{(\mathbf{T}_d)} = 5$ to a set of four *n*-pentyls, a set of four isopentyls, a set of four *t*-pentyls, a set of four 2,2-dimethyl-1-propyls, and a set of four 1-ethyl-1-propyls.

We should add a comment on the recognition of the $\mathbf{T}_d$-stereoisomers (e.g., **90**) in terms of matched and mismatched nature.[29] Because each ethyl ligand of **90** belongs to a $\mathbf{C}_s$-symmetry, it exhibits mismatched nature to the local symmetry ($\mathbf{C}_{3v}$) of the $\mathbf{T}_d(/\mathbf{C}_{3v})$-orbit for the $\mathbf{T}_d$-promolecule (**2**). Hence, the symmetry of **90** is restricted into $\mathbf{D}_{2d}$ so that the $\mathbf{C}_s$ becomes matched to the local symmetry of the $\mathbf{D}_{2d}(/\mathbf{C}_s)$-orbit. In other words, the highest attainable symmetry of **90** is $\mathbf{D}_{2d}$, which is assigned to one of fixed conformers. On the other hand, tetramethylmethane (2,2-dimethylmethane) is recognized to belong to the $\mathbf{T}_d$-symmetry even in its highest attainable symmetry. Because the methyl ligand belong to the $\mathbf{C}_{3v}$-symmetry, it exhibits matched nature to the local symmetry ($\mathbf{C}_{3v}$) of the $\mathbf{T}_d(/\mathbf{C}_{3v})$-orbit for the $\mathbf{T}_d$-promolecule (**2**).

The **T**-column of Table 2 lists the numbers of chiral centroidal alkanes corresponding to the promolecule **3** shown in Fig. 2. The four chiral proligands (p's) of the same kind in **3** are selected so that the number of **T**-alkanes of carbon content $4n + 1$ ($N_{4n+1}^{(\mathbf{T})}$) is

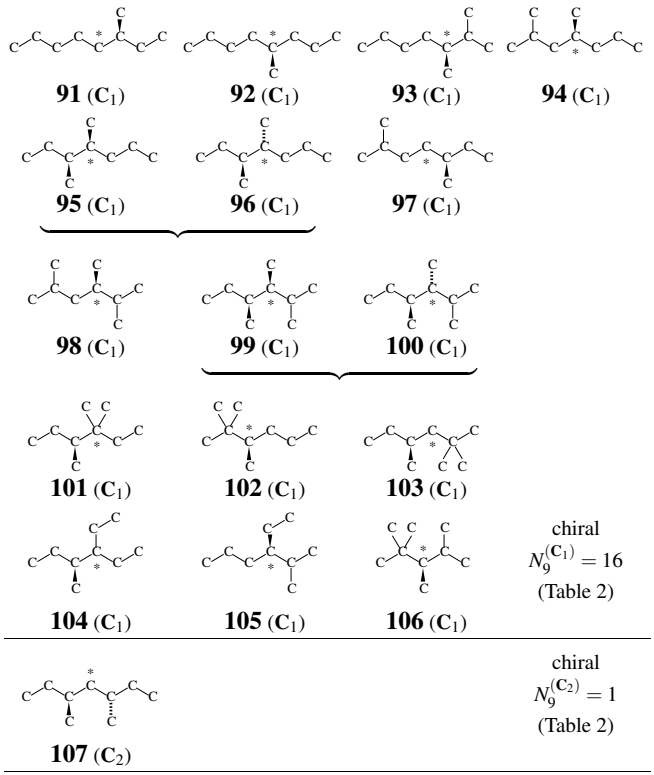

Figure 10: Symmetry-itemized numbers of chiral alkanes of carbon content 9. A wedged edge is used to show the configuration of the carbon node if necessary. Each carbon with an asterisk is a centroid.

equal to the number of chiral alkyl ligands of carbon content n. As a result, there appears the first example in the value $N_{17}^{(\mathbf{T})} = 1$ for carbon content $4n + 1 = 17$ (i.e., $n = 4$ for $m = 2n = 8$). This alkane corresponds to a set of four *sec*-butyls, each of which is the smallest alkyl ligand exhibiting chirality.

Because p_4 and $\mathrm{p}_2\overline{\mathrm{p}}_2$ exhibit the same carbon content, a **T**-promolecule (**3**) corresponds to a $\mathbf{S}_4$-promolecule (**5**) in one-to-one fashion. Hence, we obtain the following relationship:

$$N_k^{(\mathbf{T})} = N_k^{(\mathbf{S}_4)}. \tag{124}$$

This relationship is confirmed by the inspection of the $N_k^{(\mathbf{T})}$-column of Table 2 as well as the $N_k^{(\mathbf{S}_4)}$-column of Table 1. Note again that a pair of enantiomeric $N_k^{(\mathbf{T})}$-alkanes is counted just once in the present enumeration, while an achiral $N_k^{(\mathbf{S}_4)}$-alkane is spontaneously counted just once.

Let us compare the functional equation $N(x)^{(\mathbf{S}_4)}$ (eq. 60) with the functional equation $N(x)^{(\mathbf{T})}$ (eq. 65). Although the two functional equations give the same numbers as shown in eq. 124, they are different in the component terms, i.e., $c(x^4)$ vs. $b(x^4)$. The component term $c(x^4)$ is concerned with a four-membered enantiospheric orbit, while the component term $b(x^4)$ is concerned with a four-membered hemispheric orbit. The difference in their sphericities decide the chirality fittingness of the orbits so as to generate such different promolecules as the $\mathbf{S}_4$-promolecule (**5**) and the **T**-promolecule (**3**).

8.4 Fujita's PCI Method vs. Fujita's Proligand Method

Fujita's PCI method described in the present paper uses the functional equations (eqs. 56–66) based on the PCI-CFs (eqs. 2–12) for counting centroidal alkanes as well as the functional equations (eqs. 89–93) based on the PCI-CFs (eqs. 31–35) for counting bicentroidal alkanes. Thereby, the enumeration results (Tables 1, 2, and 4) are itemized with respect to the subgroups of the $\mathbf{T}_d$-point groups or of the **K**-factor groups.

On the other hand, Fujita's proligand method[26–28] uses the functional equations (eqs. 79–81) based on the CI-CFs (eqs. 13, 77, and 78) for counting bicentroidal alkanes as well as the functional equations (eqs. 108–110 and eqs. 117–119) based on the CI-CFs (eqs. 102–104 and eqs. 111–113) for counting bicentroidal alkanes. Thereby, the enumeration results are itemized with respect to achiral and chiral alkanes (Table 3) as well as with respect to centroidal & unbalanced alkanes, bicentroidal & unbalanced ones, and bicentroidal & balanced ones (Tables 5 and 6). Although the CI-CFs have been subsidiarily obtained through Fujita's PCI method in the present paper, they can be more directly obtained by using Fujita's proligand method.

As found by comparing the set of Tables 1, 2, and 4 with the set of Tables 3, 5, and 6, the itemization generated by Fujita's PCI method is more detailed than that of Fujita's proligand method. However, Fujita's PCI method requires tables of marks,[20] which are not always easy to be constructed. On the other hand, Fujita's proligand method uses the cycle structure of each permutation, which is easily obtained in general. Obviously, the easy accessibility of Fujita's proligand method is accomplished at the expense of such detailed itemization as brought about by Fujita's PCI method.

It follows that there is a trade-off between the more detailed itemization and the less availability of mark tables in Fujita's PCI method. Once a mark table is available, however, Fujita's PCI method turns out to be a versatile tool for discussing stereoisomerism comprehensively, as exemplified in the present article.

9 Conclusion

Alkanes are counted as stereoisomers or 3D-trees by means of Fujita's PCI (partial-cycle-index) method.[20, 25] where the alkanes are categorized according to the dichotomy between centroidal and bicentroidal 3D-trees. The centroidal alkanes are enumerated by using a tetrahedral skeleton of $\mathbf{T}_d$-symmetry under the criterion of defining such centroidal 3D-trees, where they are itemized in terms of the eleven subgroups of the $\mathbf{T}_d$-symmetry. On the other hand, the bicentroidal alkanes are enumerated by using a two-nodal skeleton belonging to the $\mathbf{K}$-symmetry, where they are itemized in terms of the five subgroups of the factor group $\mathbf{K} = \mathbf{D}_{\infty h}/\mathbf{C}_{\infty}$. Both the enumerations are based on functional equations derived from partial cycle indices with chirality fittingness (PCI-CFs), where the component functions $a(x^d)$, $c(x^d)$, and $b(x^d)$ (or their modifications) are substituted for three kinds of sphericity indices (SIs), i.e., a_d for homospheric orbits, c_d for enantiospheric orbits, and b_d for hemispheric orbits. Respective functional equations based on the itemization by subgroups are programmed by means of the Maple programming language. The resulting programs are executed to give respective stereoisomer numbers, which are collected in tabular forms with itemization up to carbon content 100.

We gratefully acknowledge the financial support given to our recent project by the Japan Society for the Promotion of Science: Grant-in-Aid for Scientific Research B (No. 18300033, 2006).

References

[1] Morrison, R. T.; Boyd, R. N. *Organic Chemistry (5th Ed)*; Allyn And Bacon: Boston, 1987.

[2] Fessenden, R. J.; Fessenden, J. S.; Logue, M. *Organic Chemistry (6th Ed.)*; Brooks/Cole: Monterey, 1998.

[3] Pine, S. H. *Organic chemistry (5th Ed)*; McGraw-Hill: New York, 1987.

[4] Harary, F. *Graph Theory*; Addison-Wesley: Reading, 1969.

[5] Biggs, N. L.; Lloyd, E. K.; Wilson, R. J. *Graph Theory 1736–1936*; Oxford Univ. Press: Oxford, 1976.

[6] Pólya, G.; Tarjan, R. E.; Woods, D. R. *Notes on Introductory Combinatorics*; Birkhäuser: Boston, 1983.

[7] Trinajstić, N. *Chemical Graph Theory, Vol. I and II*; CRC Press: Boca Raton, 1983.

[8] Hosoya, H. *Kagaku no Ryoiki* **1972**, *26*, 989–1001.

[9] Rouvray, D. H. Isomer enumeration mehthods. *Chem. Soc. Rev.* **1974**, *3*, 355–372.

[10] Polansky, O. E. Polya's method for the enumeration of isomers. *MATCH Commun. Math. Comput. Chem.* **1975**, *1*, 11–31.

[11] Balasubramanian, K. Application of combinatorics and graph theory to spectroscopy and quantum chemistry. *Chem. Rev.* **1985**, *85*, 599–618.

[12] Cayley, A. On the mathematical theory of isomers. *Philos. Mag.* **1874**, *47*, 444–446.

[13] Cayley, A. On the analytical forms called trees, with application to the theory of chemical combinaitons. *Rep. Brit. Assoc. Advance. Sci.* **1875**, *45*, 257–305.

[14] Henze, H. R.; Blair, C. M. The number of structurally isomeric alcohols of the methanol series. *J. Am. Chem. Soc.* **1931**, *53*, 3042–3046.

[15] Henze, H. R.; Blair, C. M. The number of isomeric hydrocarbons of the methane series. *J. Am. Chem. Soc.* **1931**, *53*, 3077–3085.

[16] Pólya, G. Kombinatorische Anzahlbestimmungen für Gruppen, Graphen und Chemische Verbindungen. *Acta Math.* **1937**, *68*, 145–254.

[17] Pólya, G.; Read, R. C. *Combinatorial Enumeration of Groups, Graphs, and Chemical Compounds*; Springer-Verlag: New York, 1987.

[18] Otter, R. The number of trees. *Ann. Math.* **1948**, *49*, 583–599.

[19] Robinson, R. W.; Harary, F.; Balaban, A. T. The enumeration of chiral and achiral alkanes and monosubstituted alkanes. *Tetrahedron* **1976**, *32*, 355–361.

[20] Fujita, S. *Symmetry and Combinatorial Enumeration in Chemistry*; Springer-Verlag: Berlin-Heidelberg, 1991.

[21] Fujita, S. The USCI approach and elementary superposition for combinatorial enumeration. *Theor. Chim. Acta* **1992**, *82*, 473–498.

[22] Fujita, S. Enumeration of digraphs with a given automorphism group. *J. Math. Chem.* **1993**, *12*, 173–195.

[23] Fujita, S. Unit subduced cycle indices for combinatorial enumeration. *J. Graph Theory* **1994**, *18*, 349–371.

[24] Fujita, S. Systematic enumeration of non-rigid isomers with given ligand symmetries. *J. Chem. Inf. Comput. Sci.* **2000**, *40*, 135–146.

[25] Fujita, S. Generalization of partial cycle indices and modified bisected mark tables for combinatorial enumeration. *Bull. Chem. Soc. Jpn.* **2000**, *73*, 329–339.

[26] Fujita, S. Graphs to chemical structures 1. Sphericity indices of cycles for stereochemical extension of pólya's theorem. *Theor. Chem. Acc.* **2005**, *113*, 73–79.

[27] Fujita, S. Graphs to chemical structures 2. Extended sphericity indices of cycles for stereochemical extension of pólya's coronas. *Theor. Chem. Acc.* **2005**, *113*, 80–86.

[28] Fujita, S. Graphs to chemical structures 3. General theorems with the use of different sets of sphericity indices for combinatorial enumeration of nonrigid stereoisomers. *Theor. Chem. Acc.* **2006**, *115*, 37–53.

[29] Fujita, S. Promolecules for characterizing stereochemical relationships in non-rigid molecules. *Tetrahedron* **1991**, *47*, 31–46.

[30] Fujita, S. Subduction of coset representations. an application to enumeration of chemical structures with achiral and chiral ligands. *J. Math. Chem.* **1990**, *5*, 121–156.

[31] Fujita, S. Systematic enumeration of high symmetry molecules by unit subduced cycle indices with and without chirality fittingness. *Bull. Chem. Soc. Jpn.* **1990**, *63*, 203–215.

[32] Fujita, S. Stereochemistry and stereoisomerism characterized by the sphericity concept. *Bull. Chem. Soc. Jpn.* **2001**, *74*, 1585–1603.

[33] Fujita, S. Promolecules with a subsymmetry of $\mathbf{D}_{\infty h}$. Combinatorial enumeration and stereochemical properties. *J. Chem. Inf. Comput. Sci.* **1992**, *32*, 354–363.

[34] Fujita, S. Combinatorial enumeration of non-rigid isomers with given ligand symmetries on the basis of promolecules with a symmetry of $\mathbf{D}_{\infty h}$. *J. Chem. Inf. Comput. Sci.* **2000**, *40*, 426–437.

[35] Jordan, C. Sur les assemblages de lignes. *J. Reine Angew. Math.* **1869**, *70*, 185–190.

[36] Monagan, M. B.; Geddes, K. O.; Heal, H. M.; Labahn, G.; Vorkoetter, S. M.; McCarron, J.; DeMarco, D. *Maple 9. Introductory Programming Guide*; Maplesoft: Waterloo, 2006.